The extreme floods in the Ebro River basin since 1600 AD

Josep Carles BALASCH[a*], David PINO[b,c], Josep Lluis RUIZ-BELLET[a], Jordi TUSET[d], Mariano BARRIENDOS[e], Xavier CASTELLTORT[a], Juan Carlos PEÑA[f]

[a]Department of Environment and Soil Sciences, University of Lleida, Rovira Roure 191, 25198 Lleida, Spain.

[b]Department of Physics, Universitat Politècnica de Catalunya·BarcelonaTech. Esteve Terrades 5, 08860 Castelldefels, Spain.

[c]Institut d'Estudis Espacials de Catalunya (IEEC-UPC). Gran Capità 2-4, 08034 Barcelona, Spain.

[d]RIUS Fluvial Dynamics Research Group, University of Lleida. Rovira Roure 191, 25198 Lleida, Spain.

[e]Department of History and Archaeology, University of Barcelona. Montealegre 6, 08001 Barcelona, Spain.

[f]Servei Meteorològic de Catalunya. Berlín 38-48 4ª, 08029 Barcelona, Spain.

[*]Corresponding author: cbalasch@macs.udl.cat Tel: +34973003736

Abstract

Reliable and complete knowledge of the historical floods is necessary for understanding the extreme hydrological dynamics of the rivers, their natural variability and anthropic changes. In this work we reconstruct the most important floods of the Ebro basin during the last 400 years in different areas of the basin. The analysis is based on four different areas: the Ebro River at Zaragoza, the Cinca River at Fraga, the Segre River at Lleida, and the Ebro River near its mouth at Tortosa.

Based on a documentary research, we have first obtained relevant information about the initial conditions (rainfall duration and distribution, snow cover influence) and the maximum flood heights that allow to reconstruct the maximum peak flows by using hydraulic models and to calculate the subbasins contributions.

The results show four main types of extreme floods: a) those affecting simultaneously all the subbasins with the highest peak discharges (Ebro at Tortosa in 1787: 0.15 $m^3s^{-1}km^{-2}$); b) those originated at the western basin, upstream from Zaragoza, with an Atlantic origin, presenting moderate maximum peak flows, caused by persistent winter rainfall and where snowmelt significantly contributes to the flood; c) those originating at the central Pyrenean subbasins, with Mediterranean origin, occurring, with high peak discharges. These mainly occur during autumn as a consequence of rainfalls of different duration (between 3 days and 1 month), and without significant snow thawing and d) finally, less frequent but very intense flash floods events centered in the Lower Ebro area with low peak flows.

In terms of frequency, two different periods can be distinguished: from 1600 until 1850, the frequency of events is low; since 1850 the frequency of events is clearly higher, due to an increase of the climatic variability during last stages of the Little Ice Age. From the 1960's reservoirs construction modifies discharges regime.

Key words: Ebro River, historical floods, peak discharge reconstruction, subbasin contributions, spatio-temporal variability

1. INTRODUCTION

The European Union regulatory framework for planning flood risk (EU Directive 2007/60/EC) uses information from previous floods obtained from hydrometric series of maximum peak flows and from documentary sources of historical floods.

Sometimes information about the largest peak flows during a flood is scarce for several reasons: they seldom occur; it could be difficult to measure hydraulical variables such as water height and flow speed; and due to the destruction of the instrumentation during the flood. However, determining this type of data with robustness and reliability is most needed for estimating the expected discharge for different return periods.

While the current requirements for the secure design of civil infrastructures must include return periods of 500 years or more, the available series do not cover even 50 years for many rivers and it is very unusual to have continuous series that are longer than 100 years for any river (Macdonald and Sangster, 2017). This clearly reflects the important lack of representativeness of the data.

On the other hand, IPCC (2013) projects an increase in extreme climatic events, including the occurrence of floods. In order to reduce the uncertainty of these projections, it is advisable to collect instrumental and documentary data covering long periods in order to explain the variability of the hydrological systems and to be able to relate flood occurrence to natural or anthropogenic causes: a) climate change, b) land use modifications at the basin scale, and c) changes in the riverbeds and reservoirs (Merz et al., 2014; Kundzewicz et al., 2014). Having broad and centuries-old knowledge of the hydrological data allows us to investigate the long-term temporal variability and the lack of stationarity in the fluvial systems (Milly et al., 2008; Machado et al., 2015).

This new necessity is clearly reflected by some early 21st century reviews of flood series at different rivers being published in journals specializing in historical hydrology and paleohydrology (Benito et al., 2005, 2015b; Gregory et al., 2006; Brázdil and Kundzewicz, 2006). There is currently an extended chronology in Europe (Glaser et al., 2010; Brázdil et al., 2006, 2012; Luterbacher et al., 2012) that allows detecting spatial and temporal

77 changes in the flood regimes (Blöschl and Montanari, 2010; Hall et al., 2014; Kjeldsen et
78 al., 2014; Kundzewicz et al., 2014)

79 For the Iberian Peninsula (IP), there are historical chronologies that cover most of the
80 basins (Barriendos and Rodrigo, 2006; Benito and Machado, 2012), the Mediterranean
81 coast (Barriendos and Martín-Vide, 1998), Catalonia (Barriendos et al., 2003; Llasat et
82 al., 2005; Barrera-Escoda and Llasat, 2015), SE of IP (Machado et al., 2011), the Atlantic
83 rivers (Benito et al., 2003), and some specific areas of the Pyrenees mountain range
84 (Corella et al., 2014, 2016).

85 Despite the quality of those previous works, we still have a reduced knowledge of the
86 magnitude (maximum peak flow) of some of the floods and this information is very
87 difficult to obtain (Herget et al., 2014, Benito et al., 2015a). During the last decade,
88 several studies have reconstructed the maximum peak flow at a particular location in a
89 particular basin (Thorndycraft et al., 2006; Balasch et al., 2007; Calenda et al., 2009;
90 Elleder, 2010). Considering the whole basin of a river, some historical analysis that cover
91 several centuries have been published (Benito et al., 2003; Naulet et al., 2005; Herget
92 and Meurs, 2010; Balasch et al., 2011; Elleder et al., 2013; Roggenkamp and Herget,
93 2014), although they do not analyze the role and contribution of the different
94 tributaries, which is fundamental to understanding the different hydrological responses
95 of the subbasins during the floods.

96 For the particular case of the Ebro River, the analysis of the hydrology regarding the
97 magnitude of the extreme floods before the instrumental period has been quite limited
98 (López-Bustos, 1972, 1981; Ruiz-Bellet et al., 2015b). The main goals of this work are to
99 reconstruct the maximum peak flow of the large floods at the mouth of the Ebro basin
100 (Tortosa) and to study and evaluate the contributions of the main subbasins (Upper Ebro
101 in the west, and Cinca and Segre rivers in the central Pyrenees), specifically at the
102 hydraulic, and hydrological levels. In addition, we seek to qualitatively study the
103 previous soil moisture conditions. This analysis will be performed on the magnitude,
104 temporal evolution (frequency), seasonality, and complementarity of the discharge
105 contributions. With this information we would like to increase our knowledge about the

temporal variability of the extreme floods in one of the most important Mediterranean rivers and to improve some aspects of planning flood risk management.

2. STUDY AREA: THE EBRO RIVER BASIN

The Ebro is one of the great rivers of the Mediterranean basin, similar in size and mean discharge to the (France and Switzerland) and Po (Italy), but smaller than the Nile and Danube. Within the IP, it is the second longest (930 km), the second in mean discharge (428 m^3s^{-1}), and the most regular in annual discharge volume.

The Ebro River drains the north-eastern part of the IP, which includes most of the southern side of the Pyrenees Range, into the Mediterranean Sea (Figure 1). It has a NW-SE orientation and a triangular-shaped basin of 85362 km^2, which approximately matches the Cenozoic foreland basin caused by the Alpine rising of the Pyrenees Range. This range delimits the basin to the N, whereas the Cantabrian Massif delimits it to the NW, the Iberian System Range to the S and SW and the Catalan Pre-Coastal Range to the E.

Regarding its morphology, the main course is divided into three parts: The Upper Ebro, from Peña Labra (Cantabria) up to Miranda de Ebro (250 km, mean slope 7.6 mkm^{-1}); the Middle-Ebro, from Haro up to Mequinenza (565 km, 480 km of them with meanders, and a mean slope 0.66 mkm^{-1}) and the Lower Ebro, between the confluence with the Segre-Cinca system up to the Mediterranean Sea (115 km, mean slope 0.46 mkm^{-1}) (Ollero et al., 2004; Del Valle et al., 2007).

Mean annual rainfall in the whole basin is 622 mm during the period 1920-2000. However, rainfall is very unevenly distributed across the basin: there is a high altitudinal gradient as well as a W-E gradient: 1000-1500 mm in the Cantabrian mountain ranges and the Pyrenees; 400-700 mm in the Iberian System range; and less than 400 mm in the central course of the Ebro, and in the lower courses of the Cinca and Segre. In the period 1950-2001 a small decrease in the amount of precipitation at the headwaters located at the Pyrenees were observed, and this was especially concentrated during the

spring and summer (Vicente-Serrano et al., 2007). Evapotranspiration losses have an opposite gradient to those of rainfall: they are higher in lower areas, with a basin average value of 450 mm. Increasing water use and changes in soil use in mountainous regions have greatly reduced runoff volume at Tortosa, near the outfall: from 18500 hm^3yr^{-1} in the 1960s to 12000 hm^3yr^{-1} (García-Ruiz et al., 1995; Gallart and Llorens, 2004). In terms of the runoff coefficient this represents a change from 35% to 22.7%.

Due to the extension and geographical configuration of the Ebro basin, there is a high climatic variability between the headwaters and the lowlands and a remarkable influence in the hydrological response due to the preceding seasonal conditions (López-Moreno et al., 2013). This translates into different hydrological regimes, according to which the Ebro basin can be divided into three great hydrological areas, that include one or more subbasins (Figure 1 and Tables 1 and 2):

- The Upper Ebro, or the western subbasin, running from the source to Zaragoza. This section lies approximately in the center of the medium reach and collects the contributions from the tributaries that have an Atlantic influence. It includes the following three types of subbasins. First, there are the rivers that have an Atlantic type of climates: the Oca, Zadoya, Najerilla and Cidacos. Next, we have the subbasins located in the NW of the Iberian System Range: the Jalón and Huerva. Finally, some western Pyrenean subbasins: the Ega, Arga, Aragón and Gállego, although this last tributary contributes downstream Zaragoza. The hydrological regime is driven by rain and snow in winter and spring.

- The southern central Pyrenees basin represented by the main Ebro tributaries: the Cinca and Segre rivers. The hydrological regime is characterized by spring snowmelt and autumn rainfalls. The Cinca and Segre can be considered twin rivers in terms of area, hydrological regime and discharge. However, they have been analyzed separately in this study.

- The Middle and Lower Ebro course, from Zaragoza to the Sea: it contains the small tributaries of the southeastern area of the Iberian System and the Catalan Pre-Coastal Range (Ports de Beseit), such as the Martín, Guadalope and

Matarraña. Rainfall is more frequent in autumn. The water budget in this area is negative due to high evapotranspiration and human use.

The result of this diverse basin is a highly complex hydrological regime in terms of variability, irregularity and seasonality of the flow. According to the climate of the area, the annual maximum instantaneous peak discharge (Qci) can occur at any time in different places within the catchment (Davy, 1975). Thus, in the western area where the Upper Ebro lies, floods generally happen in winter and spring; in the Segre-Cinca system, they happen in spring and autumn; in the upper half of the Lower Ebro, they happen in spring and summer; and in the lower half of the Lower Ebro, near Tortosa (Ports de Beseit), they happen in autumn (Figure 2).

Floods starting in the headwaters of the Ebro basin take 6-7 days to reach the sea: 2-3 days down to Miranda, 1.5-2 days from Miranda to Zaragoza, then 2-3 days from Zaragoza to Tortosa and to the sea. Floods originating in the Segre-Cinca system have a transit time of 1.5-2 days.

Throughout the 20th century, about 190 dams were built in the Ebro basin, primarily in the main Pyrenean tributaries and in the Lower Ebro (Mequinenza, Riba-roja, and Flix). The impoundment runoff index (that is the ratio between impounding capacity and annual runoff volume) is presently 57%. The Mequinenza reservoir (1966) is the largest one with a capacity of 1534 hm^3, and together with the Riba-roja reservoir (1967, 210 hm^3), these have altered the flood regime in the Lower Ebro (López-Moreno et al., 2013): they have reduced by 30% the peak flows with a return period of between 2 and 10 years (Batalla et al., 2004); and by 25% the peak flows with a return period of between 10 and 25 years (Batalla and Vericat, 2011).

3. METHODOLOGY

To fulfill the objectives of this paper –which is to the quantitatively reconstruct the hydrological response of the Ebro basin during the most extreme floods of the last 400 years– it was necessary to separately compile the peak-flow series in the four main subbasins: The Upper Ebro, Segre, Cinca and Lower Ebro (whole Ebro). Furthermore, in order to assess the cause of each flood, meteorological and hydrological information is

192 also needed: rainfall extension and duration; soil saturation (estimated from rain events
193 in previous days) and snowmelt runoff. All this information is obtained from the sources
194 listed in Table 3, all of which are part of the PREDIFLOOD/AMICME database (Barriendos
195 et al., 2014) that includes 1524 flood events that caused 4244 documented cases of
196 damage.

197 A site in each subbasin was selected for compiling the peak-flow series. This selection is
198 based on two factors: first the availability of information about discharge data series and
199 historical floods at the site; and, second, its proximity to the subbasin's outlet. The
200 selected sites were the towns of Zaragoza (Upper Ebro), Fraga (Cinca), Lleida (Segre) and
201 Tortosa (whole Ebro basin). For each site, in order to select the major floods, we defined
202 a discharge threshold by calculating the minimum peak discharge that floods the old
203 town and causes structural damages. The hydrological characteristics of these control
204 subbasins are shown in Table 2. The compiled peak-flow values can be divided into three
205 classes, depending on the information use to obtain them:

206 • Measured peak flows: obtained from official gauging data series.

207 • Reconstructed peak flows: when it doesn't exist a measured peak flow but there
208 is an observed maximum water height.

209 • Estimated peak flows: for floods that have no measured peak flow nor observed
210 maximum water height, as in the case of five floods at Fraga in the Cinca
211 subbasin.

212 Regarding the measured peak flows, systematic flow gauging in the Ebro basin started
213 on 1913 in the towns of Zaragoza and Tortosa (Ebro River) and as well as in Lleida (Segre
214 River) and it began in 1928 in Fraga (Cinca River). Many of the gauging stations across
215 the basin have accumulated close to 100 years of data. Unfortunately, peak-flow
216 measurements are scarce: there are no flow measurements of any flood prior to the
217 20th century and, within that century, most of the systematic measurement series are
218 missing the greatest floods, such as 1907, 1937 and 1982.

219 The reconstructed peak flows have been either obtained from the literature or
220 calculated *ad hoc* for this paper. In this last case, the reconstruction method is based on
221 hydraulic modeling from the observed maximum water height (Figure 3), as explained
222 in Benito et al. (2004), Lang et al. (2004), Remo and Pinter (2007), Calenda et al. (2009)
223 and Balasch et al. (2011). Aside from information about observed water height, this
224 reconstruction method requires data about the hydraulics (that is, the geometry and
225 roughness of the river bed and flood plain) at the time of each reconstructed flood (Table
226 4). These data (observed maximum water height and geometry and roughness of the
227 river bed) are obtained from historical documents such as epigraphic marks, maps,
228 engravings, chronicles, and historical accounts (Table 3). The software used to model
229 the floods is: HEC-GeoRAS, v.10.1 (USACE, 2010a), HEC-RAS v.4.1.0 (USACE, 2010b) and
230 IBER v.2.4 (Bladé et al., 2012, Table 4).

231 The models were calibrated at each site by using measured peak flows. The flood on
232 1961 was used to calibrate the models at Zaragoza and Tortosa (Xerta) and the 1982
233 flood in Fraga and Lleida. For the case of Tortosa, the model was actually applied at the
234 scale of the Sant Marti church at Xerta (Figure 3d). This could be done because the
235 richness and reliability of the Xerta scale. The distance between Xerta and Tortosa is
236 small (10 km) and the basin is only 0.2% larger and, as a consequence, the damping
237 effect is negligible and the discharges calculated at Xerta could be directly extrapolated
238 to Tortosa.

239 The five estimated peak flows for the Cinca subbasin were obtained by subtracting the
240 Upper Ebro and Segre subbasins peak flows from the peak flow at Tortosa after the
241 proper routing of the flows. Comparisons were made of the hydrographs of the 1930,
242 1961, 2003 floods at Zaragoza and Tortosa, on the one hand, and of 1982 at Lleida and
243 Tortosa, on the other hand, in order to estimate the routing parameters of the peak
244 flows (travel time and wave attenuation). In addition, different order magnitude floods
245 were modeled in a 150-km long reach in the Lower Ebro subbasin with IBER v.2.4 to
246 quantify the flood lamination downstream Zaragoza.

247 Both peak-flow reconstructions and estimations are less accurate than direct
248 measurements. Reconstructed peak-flow errors are around 10% when the hydraulic

model could have been calibrated with a recent, well-known flood and they are around 50-80% when such a calibration was not possible (Barriendos et al., 2003; Benito et al., 2004; Gaume et al., 2004; Lang et al., 2004; Ruiz-Bellet et al., 2017). There are no quantifications of the error of peak-flow estimations from water budgets, but they must be undoubtedly larger than those of the reconstructions.

4. RESULTS

The chronological study of the long series for historical flooding long series in the study areas (except Fraga) was started by Barriendos and Martín-Vide (1998), Llasat et al. (2005) and Barriendos and Rodrigo (2006), all of whom prepared the first catalogue on the severity and extension of the different cases (292), but without quantifying the magnitude of the peak discharges, the spatial distributions or the persistence of the rain.

In this section we will first describe the events by subbasins and for the whole basin at Tortosa. Secondly, the most relevant events of the historical period for the whole basin will be shown. Finally, the floods will be classified according to different spatial patterns and considering the meteorological and hydrological processes involved in the subbasin.

4.1 Floods at the subbasins

4.1.1 Upper Ebro subbasin (western basin up to Zaragoza)

It's important to note that during the analyzed period 7 floods with peak flows greater than 3500 m^3s^{-1} occur at Zaragoza (Figure 4a, Table 5); most of them since 1850 (Ruiz-Bellet et al., 2015b).

Between 1600 and 1750 there was only one large flood (1643), which largely affected the bridge. The estimated peak flow of 5560 m^3s^{-1} is considered to be the record in the Zaragoza register. Two documented smaller floods at cities located at the upper basin (1636, 1670) do not seem to have occurred at Zaragoza. During a second short period (1750-1800), two large events occurred 12 years apart, 1775 and 1787 (with peak flows of 5180 and 4600 m^3s^{-1}, respectively). Since 1850, the occurrence of floods increased. In 1871, the latest large flood occurred with a peak flow of 4844 m^3s^{-1}. From this moment

277 on, smaller floods happened, with the most important episode of the 20th occurring in
278 1961, with 4130 m^3s^{-1}.

279 In summary, three first-order floods occurred at Zaragoza between 1600 and 1850, that
280 is, 1.2 events per century with very important peak flows. Since 1850, 4 extreme floods
281 (over-threshold) have occurred (2.7 per century), but with less severity. The maximum
282 specific peak discharge at the Zaragoza section is 0.13 $m^3s^{-1}km^{-2}$.

283 **4.1.2 Cinca River at Fraga subbasin**

284 The reconstructed series of maximum peak flow of the Cinca River at Fraga includes peak
285 discharges above 2500 m^3s^{-1} and has a heterogeneous quality, especially for the oldest
286 floods (Figure 4b, Table 6). Taking into account the severity of the analyzed damages,
287 during the 17th century and the first half of the 18th, they are not large floods compared
288 to the following centuries. However, at the beginning of the 17th century was the
289 November 1617 event, which is reported by several documented sources to have
290 affected the east side of the Ebro basin, including Fraga (Thorndycraft et al., 2006).
291 Calculations show that, despite the duration of the episode (it rained for approximately
292 one month), the maximum peak flow for this event would be around 2500 m^3s^{-1}, lower
293 than subsequent registered maximum peak flows during other episodes. Between 1750
294 and 1850, there are 2 important floods (1787, 1788) and one of second order (1762).
295 The most important flood in the Ebro basin, occurred in October 1787, is not
296 extraordinary at Fraga. Documents describe this flood as smaller than the flood of
297 September 1788, when the historical peak flow maximum at Fraga was reached with
298 4500 m^3s^{-1} (or 0.47 $m^3s^{-1}km^{-2}$). There is no record of this flood at the mouth of the Ebro
299 (Tortosa) due to the damping of the flow during its routing and the lack of contributions
300 from other subbasins.

301 During the second half of the analyzed period (1850-2010), there are six episodes with
302 a peak flow of around 2500 m^3s^{-1} or higher (1853, 1866, September 1874, 1907, 1937,
303 and 1982), that is, four per century; the most intense period is between 1850 and 1910
304 with four episodes having peak flows of between 2500 and 3900 m^3s^{-1}. Surprisingly, the
305 second largest maximum peak flow occurred in November 1982 (4200 m^3s^{-1}) when the

306 reservoirs had already been built; and the third one occurred in October 1907 (3900 m^3s^{-1}).

308 **4.1.3 Segre River at Lleida subbasin**

309 The historical and recent floods registered at the Segre River at Lleida in the period 1600-
310 2017 comprises 14 events (Figure 4c, Table 7). We have selected the 9 floods with a
311 maximum peak discharge greater than 3000 m^3s^{-1}, which is the threshold flow necessary
312 for flooding the right bank of the city. Between 1600 and 1850 there is a low frequency
313 of extreme events: there are only 3 episodes (1.2 per century). This period starts with
314 the episode in November 1617 (Thorndycraft et al., 2006), which produced catastrophic
315 damages in the basins of eastern Catalonia, but it was not as important in the Segre
316 basin, with a maximum peak flow around 4000 m^3s^{-1}, being a second order event for this
317 basin. However, the more exceptional episode in this period occurred in October 1787,
318 with a maximum peak flow of around 8500 m^3s^{-1} (or 0.75 $m^3s^{-1}km^{-2}$) which represents
319 more than 100 times the mean instantaneous peak flow for this section.

320 From 1850, there is an increase in the number and magnitude of the episodes. During
321 this period, there are 6 events with more than 3000 m^3s^{-1} (4 per century). Despite this
322 fact, it can be clearly observed from mid-20th century onward that the influence of the
323 reservoirs in this basin, damping the peak flows. For instance, during the large flood of
324 1907, none of the reservoirs had been built yet and the maximum peak flow at Lleida is
325 5250 m^3s^{-1}. In contrast, the floods in October 1937 and November 1982 had maximum
326 peak flows of 3600 and 3400 m^3s^{-1}, respectively, which were damped by the
327 constructions for regulating flow, influencing especially the latest episode.
328

329 **4.1.4 Lower Ebro subbasin (Ebro River at Tortosa)**

330 The flood record of the Ebro at Tortosa is based on the flood marks at Xerta and the
331 database at Tortosa, Móra d'Ebre, and Benifallet. It supposedly includes the 9 largest
332 floods that have occurred since 1600 (Figure 4d, Table 8). For all of them, the maximum
333 peak flow is above 4500 m^3s^{-1}. Consequently, we have near the river mouth, a complete
334 and trustworthy register of the large floods over the last 400 years (Ruiz-Bellet et al.,
335 2015b).

At this point, there is a first period (1600-1850) characterized by the low frequency of events with maximum peak flows greater than the threshold (2 events, 0.8 events per century). From 1620 to 1750, there is not any maximum peak flow greater than 4500 m^3s^{-1}. Then, in October 1878, occurred the flood with the largest maximum peak flow of the studied period: the flood on October 1787. The maximum peak flow at the final section of the Ebro River is estimated to have been around 13000 m^3s^{-1} (or 0.15 $m^3s^{-1}km^{-2}$), which occurred at some hydraulic obstructions at some gorges along the lower course: at the Pas de l'Ase and at the Barrufemes gorges, which can be estimated from several flood marks at different locations (Abellà, 2013).

On the other hand, there is a clear increase in the number of episodes (7, 4.6 events per century) since 1850. Ever since the construction of reservoirs around the mid-20th century near the Pyrenees and along the middle course of the Ebro, there has been a reduction in the magnitude of the maximum peak flows at Xerta, where they hardly surpass 4500 m^3s^{-1} (for instance, in 1982, when the central Pyrenees basins are largely affected but only 3780 m^3s^{-1} was registered at Tortosa). After the flood of 1787, the largest peak flows correspond to the events in 1907 (10500 m^3s^{-1}) and 1937 (9250 m^3s^{-1}).

4.2 The whole Ebro basin. The largest floods and origin

Table 9 shows the results for the 16 largest floods registered for the Ebro River and its tributaries during more than 400 years (1600-2017), including all floods above the threshold in the subbasins and the most remarkable secondary floods (1930 and 1982), and indicating also the method of determination of the maximum peak flow: systematic register, hydraulic reconstruction or hydraulic budget.

Additionally, for each analyzed flood and with the documented sources included, Table 10 shows the role played by previous rainfall episodes that may have an influence on initial soil moisture conditions, the occurrence of precedent floods and the existence of snowmelt.

The most significant episodes during the studied period in the whole basin, are classified according to their magnitude, with a maximum peak discharge at Tortosa greater than 7000 m^3s^{-1} and they are:

1. 1787 (7-9 October). This affected the whole Ebro basin. It was the episode with the highest peak flow at Tortosa (12900 m^3s^{-1}) and Lleida (8500 m^3s^{-1}), being of the first order at Zaragoza (4500 m^3s^{-1}) and having a secondary relevance at Fraga. No influence of snow thaw has been found in the documentary sources. It was produced by 10-12 nearly consecutives days of rain caused by 2 very active low-pressure areas that were blocked by a large high-pressure system moving between Scandinavia and the Balkans, combined with warm and moist air coming from the Mediterranean Sea – according to the interpretation of historical barometric data.
2. 1907 (23-24 October). This episode registers as the second highest peak flow at Tortosa (10500 m^3s^{-1}) and the third highest at Lleida (5250 m^3s^{-1}) and at Fraga (3900 m^3s^{-1}). In the western basin, the flood reaches 2900 m^3s^{-1} when Gállego River tributes the Ebro River downstream Zaragoza. It was generated by a passing front that produced moderate to severe precipitation in the Pyrenees after an unusual episode of persistent precipitation after the end of September. Snowmelt does not seem to have played any role.
3. 1937 (28-29 October). The maximum peak flow at Tortosa was 9250 m^3s^{-1}, and it was produced by similar contributions from the Segre at Lleida (3600 m^3s^{-1}), the Cinca at Fraga (2600 m^3s^{-1}) and the Ebro at Zaragoza (3020 m^3s^{-1}). It was produced by a front passage crossing over the Pyrenees and producing three days of intense precipitation (Pino et al., 2016). Again, the snow contribution isn't documented. For this event, some regulation of the flow of the Segre River has to be considered by the reservoirs in Tremp and Camarasa.
4. 1853 (24-25 May). Maximum peak flows were 8250 m^3s^{-1} at Tortosa, 6000 m^3s^{-1} at Lleida and around 3000 m^3s^{-1} at Fraga. There is no flood in the western basin. For this case, snow thaw due to rain, high temperatures and the soil saturation played an important role. Previous rains are documented during the same month, and a low-pressure system centered over Catalonia sent a humid and

warm air mass from the Mediterranean Sea causing severe precipitation that enhanced snow melting at the headwaters of the basin.

5. 1866 (21 October). Several rainy days produced a maximum peak flow of 7750 m^3s^{-1} at Tortosa, coming from the Segre (5000 m^3s^{-1}) and Cinca (3000 m^3s^{-1}). Soils of the basin presented large moisture due to continuous rainy days. No snow accumulated at the headwaters of the basin, and no flooding was recorded in the western basin (Upper Ebro).

6. 1617 (8 de November). After several days of persistent rain over the NE IP and the Pyrenees after the end of September, severe precipitation occurred between 2 and 4 November, thus producing maximum peak flows at the Segre (4000 m^3s^{-1}) and Cinca (2500 m^3s^{-1}) with a maximum peak flow of 7500 m^3s^{-1} at Tortosa. In contrast, there are no flood records at Zaragoza. The role of snow thaw in this episode is unclear, but with some probability of occurrence.

The temporal analysis allows us to distinguish two different periods:

1) A first period between 1600 and 1850 characterized by a low frequency of events, two clear minima in the periods 1650-1750 and 1790-1850, with no extraordinary floods in these two periods. In between these two periods occurred the flood of October 1787, which is the event with the highest maximum peak flow in the Ebro basin not only during the analyzed period but probably also over the last millennia, if we consider the information provided by the flood marks (Miravall, 1997b). Moreover, before these two periods, another episode with the second largest extension occurred in November 1617.

2) From 1850, the frequency of the floods increases two or threefold. At the end of this period, around 1950, we can observe a reduction in the magnitude of the maximum peak flow due to construction of several reservoirs in the Pyrenees and along the middle basin of the Ebro River. Except for the floods of 1787 at Lleida, and 1788 at Fraga, it is during this second period when these tributaries present larger maximum peak discharges.

4.3 Spatial patterns of the floods and seasonality

It can be concluded from Sections 4.1 and 4.2 that, for the largest three floods (1787, 1907 and 1937), the maximum peak discharges calculated at Tortosa were due mainly to the contribution of all formative subbasins, but with a larger contribution of the central Pyrenean ones (Segre and Cinca). Despite the amount of precipitation, this fact can be explained by taking into account the location of these rivers, which are much closer to the mouth (130-150 km), and the large flow created by the slope of the basins on the southern side of the Pyrenees. The synchronicity of the maximum peak discharge of the two analyzed central Pyrenean basins can reach up to 10000 m^3s^{-1}. In contrast, the floods coming from the western basin (Upper Ebro) can have maximum peak flows at Zaragoza of around 5000 m^3s^{-1} and the flow needs to travel along the basin to reach Tortosa (340 km of a meandering pathway). As a consequence, the floods at Tortosa that do not receive a significant contribution from the Pyrenean subbasins, and they therefore present lower maximum peak flows (lower than 4500 m^3s^{-1}). For the rest of the floods, the contribution of the subbasins was quite different for each flood: Atlantic (Upper Ebro River) or Mediterranean (central Pyrenees and Lower Ebro).

Taking into account the atmospheric processes that produced the floods, it is important to note that – with the exception of 1853 flood – the largest floods occurred during autumn, and only due to extreme and persistent (from 3 days to one month) precipitations, especially over the headwaters at the Pyrenees (Pino et al., 2016). It is surprising to the traditional interpretation of events that snowmelt has no influence on most of Pyrenean floods. In contrast, during the event on 1853 snowmelt contributed largely to the flood (Table 10).

Considering the whole system (16 floods), the results clearly show four different flood patterns regarding the area where precipitation originates and concentrates:

a) Floods affecting the whole Ebro basin
b) Floods generated at the Upper Ebro basin
c) Floods generated at the central Pyrenean tributaries
d) Floods generated at the lower course of the river

Pattern a) The floods affecting the whole basin includes the events in 1787, 1907 and 1937 (18.7% of the analyzed), all of them occurring in autumn and where snowmelt did

not play any role. Surprisingly, these floods do not affect sites located upstream Zaragoza, such as, Miranda de Ebro or Logroño. This can be explained because there is a direct influence of the western Pyrenees (Ega, Arga and Aragón Rivers) and central Pyrenees (Segre and Cinca Rivers), but without any contribution from the Ebro headwaters.

The 13 remaining events are generated mainly in only one area of the basin (either the Upper Ebro basin, central Pyrenees or the lower course) with zero or small contributions from the other areas. This fact indicates that it is very unlikely to have intense frontal precipitation affecting the whole basin. Consequently, there is a clear distinction between frontal episodes coming from the Atlantic and affecting mainly the Upper Ebro River up to Zaragoza and others originating at the Mediterranean Sea that affected the central Pyrenean basins or, more rarely, the lower areas of the Ebro basin.

Pattern b) The floods that affect only the Atlantic side of the basin, in the west and up to Zaragoza, including the western Pyrenean subbasins, represent 37.5% of the analyzed floods (6). Most of them (83%) occur during winter and less often during spring (17%). This pattern includes the largest floods at Zaragoza in 1643 (4500 m^3s^{-1}), 1775 (5000 m^3s^{-1}), 1871 (4850 m^3s^{-1}), January 1874 (3624 m^3s^{-1}), and 1930 (3600 m^3s^{-1}), all of which had small consequences at Tortosa because there was not any contribution from the rivers on the northeastern side of the basin. In contrast, the flood in 1961 (4130 m^3s^{-1}) had a slightly larger maximum peak flow in the lower course of the river (4580 m^3s^{-1}), despite not having any contributions from the central Pyrenean rivers. Taking into account that these floods in the western part of the basin occur during winter and spring, they are characterized by high runoff increased by snowmelt (1643, 1871, 1930, 1961 and probably January 1874) and more rarely, without any previous snow cover (1775), as it appears in the historical sources and modern reports. These are floods with a slow response time of the basin, meaning that they need between 48 to 72 hours to reach Zaragoza and around one week to reach Tortosa.

Pattern c) This pattern concerns the Segre and Cinca subbasins (central Pyrenees) and represents 31.3% (5) of the analyzed floods. Among these, 60% occur during autumn and the rest in spring or winter. This pattern includes the floods in 1617, 1766, 1853, 1866 and 1982. Due to the seasonality of these floods, snowmelt plays no role in producing the floods; this is an important difference when comparing them with the

western subbasin. They present a sharper hydrograph when compared with pattern b). At Tortosa the peak flow includes main contributions from the Segre River, followed by the Cinca and the western part of the basin. These floods would be caused by continuous precipitation for several days (in some cases more than 10) produced by frontal systems passing over the area and fed by Mediterranean mesoscale convective systems. Due to the slope of the Pyrenean basins (> 8mkm^{-1}) and the distance between the headwaters of the rivers and the Ebro, they need 24-36 hours to reach the Ebro.

Pattern d) The final type of floods is represented by two events that occurred in the Lower Ebro and its vicinity: September 1874 and September 1884 (12.5%). The event in September 1874 is known as the Santa Tecla flash-floods (Balasch et al., 2010; Ruiz-Bellet et al., 2015a), and it was an extraordinary flash flood of convective origin over the tributaries of the lower course of the Segre and at the Lower Ebro depression where large peak flows are produced and, as a consequence, it is included here. The flood in September 1884 (Ebro at Tortosa: 6500 m^3s^{-1}) occurred only in the Lower Ebro tributaries, and the flood wave's proximity to the Ebro's final course helped to avoid routing losses. In this event, precipitation was restricted to the area of Ports de Beseit mountain range, on the SE-side of the Iberian Mountain Range and in the Lower Ebro depression. Due to the proximity between the precipitation area and Tortosa, these floods propagated quickly (1-2 days), similar to a big flash-flood even though the maximum peak flows were not among the highest ones. The precipitation producing the flood was intense and of short duration (less than 24 hours), which is related with deep convective systems of Mediterranean origin.

Regarding the seasonality of the floods as a function of the subbasin (Figure 5), we can observe clear differences between the Upper Ebro basin and the central Pyrenean ones. While the extreme floods at Zaragoza occur mainly during winter, floods at Fraga and Lleida are more frequent during autumn. At Tortosa, floods occur especially during autumn and with less frequency in winter, pointing out again the importance of the central Pyrenean tributaries.

5. DISCUSSION

5.1 Uncertainty of the results

519 The uncertainty of the results depends on the uncertainty of the input data and of the
520 hydraulic models. Regarding the historical input data, historical accounts used here are
521 quite heterogeneous, having different data quality. The more complete and checked
522 records are Tortosa and Lleida. The Zaragoza and Fraga records need additional work for
523 studying the original sources which limits the capacity to generate results. When
524 reconstructing flood series, we will always have uncertainty about the completeness of
525 the sources regarding the episodes that occurred during the studied period (Barriendos
526 et al., 2014). The dates obtained for the episodes are absolutes and very precise and the
527 reliability and precision of the floods marks are included in the corresponding tables.
528 Reliable epigraphic references of the maximum flood heights have an irregular spatial
529 and temporal distribution. They do not cover all the studied period: the oldest ones are
530 from 1617 at Tortosa (Xerta), 1787 at Lleida, and 1775 at Zaragoza, and the scarce flood
531 marks that are known at Fraga are largely uncertain. This implies that the information
532 generated is quite heterogeneous and, consequently, needs to be completed in the
533 future, especially for the Cinca River at Fraga.
534 In relation to the models, the greatest source of uncertainty is the geometry of the
535 modeled reach, since, in some cases, it may have changed considerably in the last four
536 centuries. This uncertainty is kept to a minimum by using ancient maps and
537 contemporary etchings. Besides, in some cases, the existence of old bridges' remains is
538 used to confirm the minimum changes in the geometry due to erosion and deposition
539 of sediments (cases of Zaragoza, Fraga and Lleida). Moreover, the resolution of the
540 Digital Elevation Model and the number of cross sections (in the case of HEC-RAS) are
541 considered sufficient to obtain reliable results. Model uncertainty is also reduced with
542 the calibration with modern day floods of known peak flow and water height at
543 Zaragoza, Lleida, Fraga and Tortosa. Uncertainty for modeled peak flows of extreme
544 floods in Tortosa has been estimated at 30% (Ruiz-Bellet et al., 2017).
545 This uncertainty can be greater in the case of Fraga, where, due to the scarcity of
546 information, many of the reconstructed peak flows are obtained by subtracting from the
547 flow at Tortosa the routed contributions of the other two tributaries (Upper Ebro and
548 Segre). In any case, peak-flow routing results obtained independently from the
549 comparison of known hydrographs at Zaragoza, Lleida and Tortosa and from a 3000 m^3s^-

550 [1] and a 5500 m^3s^{-1} flood modeling in a 150 km long reach are consistent and they reveal
551 that, between Zaragoza and Mequinenza, peak flows have virtually no lamination (< 5%).
552
553 **5.2 Comparison of discharge magnitudes**
554 Despite the Ebro being a western Mediterranean river, the maximum specific peak
555 discharge of the flood series at Tortosa (0.15 $m^3s^{-1}km^{-2}$) is slightly higher than the largest
556 values registered for some European rivers of similar size in moister regions: the Po at
557 Pontefagooscuro (Italy) with 0.14 $m^3s^{-1}km^{-2}$, the Danube at Wien (Austria) with 0.13 $m^3s^{-1}km^{-2}$, the Rhône at Beaucaire (France), at around 0.12 $m^3s^{-1}km^{-2}$, and the Neman at
559 Smolnikai (Russia), with 0.08 $m^3s^{-1}km^{-2}$ (Stanescu, 2004). However, the maximum peak
560 discharge at Tortosa is far from the maximum value registered in 1970 on the Narmada
561 River at Gurdeshwar (India): 0.79 $m^3s^{-1}km^{-2}$. This is the world record for maximum peak
562 discharge in any basin of comparable size (Herschy, 2003).
563
564 **5.3 Meteorological and hydrological mechanisms of flood generation**
565 Table 10 includes the initial soil moisture conditions of the subbasins produced by
566 previous rainfall, occurrence of floods in nearby dates, and the availability of a snow
567 cover, while Table 11 summarizes the affected subbasin in relation to the whole system
568 and the flood generating processes involved. According to this information, we classify
569 the flood generating mechanisms in four groups:
570
571 1. **Persistent precipitation**. Precipitation lasts more than 10 days for some episodes
572 occurring during autumn and winter. The most iconic events occurred in 1617,
573 1766, 1775, 1787, 1866 and 1907. These events are the final stages of previously
574 very wet periods that already generated problems of excessive moisture during
575 the harvest (see Table 10). These floods are generated by saturation-excess
576 overland flow due to the complete soil profile saturation after the progressive
577 accumulation of water with a slow response, but involving important runoff
578 volumes and no significant role played by snow thaw.
579 2. **Persistent precipitation and snowmelt**. It includes the events in 1643, 1853,
580 1871, 1930, 1961, and probably January 1874. They present the largest runoff
581 volumes, as can be seen in the existing hydrographs of 1871 (Galván et al., 2013),

1930 and 1961 (Marcuello, 2001). These were caused by persistent precipitation, but with saturation overland flow by snowmelt also remarkable (Table 10). Most of these events occurred at the western side of the basin, upstream Zaragoza, except 1853. In other words, snow is an important hydrological factor in the western Ebro basin, but it is not important on the Mediterranean side of the basin.

3. **Short, intense precipitation**. For the events on 1937 and 1982 precipitation only lasted 3 days and fell over dry soils and without any snow. During these episodes intensity of the precipitation reached high values during some hours (> 200 mm in 24 h, Table 10) producing hortonian (infiltration-excess) overland flow in many areas, which added to the saturation-excess overland flow. They produced intermediate runoff volumes.
4. **Extremely short intense precipitation**. A fourth group of episodes present a much more intense hydrological response; the floods occurred in September 1874 (Santa Tecla), and in 1884. These are flash floods but occurring over a large area. They are caused by short precipitations (less than one day), but they are very severe as can be concluded from the documentary sources. The hydrological response of flash floods was caused mainly by an hortonian overland flow and scarce runoff volume.

5.4 Perspectives in a global paleoclimatic framework

The temporal analysis of the hydrological extremes indicates that there is no clear regularity, but they appear to be concentrated in different periods that are associated with the climatic variability related to changes in the global atmospheric circulation, which itself is forced by different drivers, such as, solar radiation, volcanism, changes in the latitude of the north-Atlantic thermohaline circulation, greenhouse gases, among others. Climatic variability might play a major role in enhancing the intensity of the most extreme events rather than enhancing the ordinary ones (Knox, 2000) or during periods of rapid climate change (Macklin et al, 2006).

Part of the analyzed period (1600-1850) corresponds with the second half of the Little Ice Age (LIA), a climatic period characterized by high humidity, and a decrease in average temperatures of around 1^{o}C with respect the current average (Oliva et al., 2018). During

614 this period, there is greater volcanic activity, lower solar radiation, and a southern
615 movement of the North-Atlantic thermohaline circulation, which is related to the NAO.
616 As explained above, in the Ebro basin, the period 1600-1850 is characterized by a low
617 frequency of events, but with one maximum (1760-1790) and two clear minima (1650-
618 1750 and 1790-1850). During the maximum, which is related to the Maldá Oscillation
619 that is characterized by a series of droughts and floods (1760-1800, Barriendos and
620 Llasat, 2003), large floods occurred in the Segre (1766), in the Upper Ebro (1775) and in
621 the western and central Pyrenean subbasins (1787). The first minimum of floods (1650-
622 1750) occurred during the cold period of the Maunder Minimum. This is a rainy period
623 that lacks extreme phenomena due to low convectivity, and this is consistent with a
624 decrease in drought and flood frequencies recorded in Catalonia (Barriendos, 1997). The
625 second minimum (1790-1850) might be related to the cold period of the Dalton
626 Minimum, when a long drought period also occurred (1812-1825) (Prohom et al., 2016).
627 Following 1850, the frequency of extreme events is doubled or tripled, especially during
628 the period 1850-1885. This can be explained by: a) an increase in atmospheric instability
629 that produced severe precipitations at the end of the LIA (Oliva et al., 2018); and b) an
630 increase in the exposure of the population in the flooding areas, and this is tied to an
631 increase of the agricultural activity and population growth. Previous authors (Barriendos
632 and Martín Vide, 1998; Llasat et al., 2005; Benito et al., 2008; Machado et al., 2011;
633 Barrera-Escoda and Llasat, 2015; Corella et al., 2016; Oliva et al., 2018) have pointed out
634 a similar behavior of different rivers in the IP during the same periods. Since 1950, the
635 number of extreme floods decreases not only because there is a small decrease in the
636 amount of precipitation at the Pyrenees at headwaters (Vicente-Serrano et al., 2007),
637 but also because of the volumes of the flood retained in the different reservoirs.
638 Considering the whole Mediterranean basin during the last 2000 years, we can observe
639 different phases with major flood activity, occurring the last one between 1750 and
640 1800, when cold and humid climatic conditions prevailed, and two periods with low
641 frequency around 1600 and 1825 (Luterbacher et al., 2012). Sheffer et al. (2008) also
642 pointed out that floods in France were more intense during the 18th than during the
643 20th century.
644 Regarding the relation between the floods in the Ebro basin, the synoptic configurations
645 and the general circulation modes, the most extraordinary floods occurred during last

stages of the LIA (1870-1940) and they are related with a negative phase of NAO and a positive phase of the Scandinavian pattern. This is characterized by an anticyclonic blocking over the Scandinavian Peninsula that produces a wavy pattern of the jetstream and low-pressure systems, that would be intensified in the Mediterranean area, producing high convectivity. On the contrary, the floods during the warm period (1940-2010) are related with a positive phase of the NAO and negative of the Scandinavian pattern. This might produce west flows over the IP that favors the occurrence of cold fronts related with medium or low convectivity (Peña et al., 2017).

5.5 Future projections and scenarios

Climate change models (IPCC, 2003) project variations on the floods in the Mediterranean river basins in regard to on three different aspects: 1) climatically; 2) changes in the land use of the basin and riverbanks, and 3) infrastructures (Hall et al., 2014). We expect to observe a reduction in the total annual precipitation in the Ebro basin and in the number of extreme events (Vicente-Serrano et al., 2007). On the other hand, torrentiality might increase in some specific areas.

Regarding the changes on land use, it is presumed that, if temperatures increase, snow thaw would appear at the end of the winter, thus enhancing soil saturation and the winter base flows in the western basin. This would coincide with the season of maximum precipitation and therefore produce an increase of runoff volumes. The role of the changes in land use on the floods has been largely discussed (Andreassian, 2004). Although some studies show changes in the forest cover at the headwaters (González-Sampériz et al., 2017), this fact cannot be directly related to a change in flood frequency or intensity, especially for large basins (Calder and Aylward, 2006).

During the 20th century it occurred a reduction of the dimensions of the bedchannel and the decrease of the area of the flood plains at the mid-course of the Ebro River (Magdaleno and Fernández-Yuste, 2011) Nevertheless, an effort to reconnect flood plains that were disconnected in the past by the constructions of levees in the mid and lower course of the river is advisable to recover their damping natural role (Ollero, 2010). On the other hand, regarding the river channels and banks, there is no new large reservoir projected in the area to reduce the impact of the floods. Moreover, an increase

677 of population is also projected for the urban areas, producing more exposition and
678 vulnerability in flood prone areas.
679 Due to the superposition of these factors, which influence floods in opposite directions,
680 it is difficult to determine whether recent climate warming has any influence on the
681 occurrence of the floods in the Mediterranean basin, an area that was particularly
682 affected by anthropic changes during the 20th century (Luterbacher et al., 2012), but
683 probably the climatic factor will be dominant.
684
685 **6. CONCLUSIONS**
686 We have hydraulically reconstructed the maximum peak flows of the major floods at the
687 mouth of the Ebro River (Tortosa) during the last 400 years, and this has allowed us to
688 determine the contributions of the main subbasins (Upper Ebro, Cinca, Segre and Lower
689 Ebro) according to their magnitude, flooding periods, seasonality, complementarity of
690 their contributions, and the role of previous rainfall and snowmelt. Although this is an
691 initial global evaluation, the results provide us a quantitative hydraulical and
692 hydrological scheme about how the historical extreme flood events behaved in a first-
693 order Mediterranean basin during the last 400 years.
694 Regarding the spatial pattern, during the analyzed period, there is only three events
695 affecting the whole basin (1787, 1907 and 1937). Most of the episodes affect only to
696 one part of the basin: the western area, (upper and middle Ebro courses); the central
697 Pyrenean tributaries; or, very rarely, only the Lower Ebro basin. For each of these areas
698 the main hydrometeorological factors controlling the occurrence the most extreme
699 floods are different.
700 a) In the floods generated in the Upper Ebro basin during winter, long lasting
701 rainfall (10-30 days) and snow thaw play a major role. These are floods having a
702 higher hydraulic path: more than 300 km of meanders with small slope channels
703 along the middle and lower courses of the river.
704 b) Episodes with the highest peak flows originate in the central Pyrenees (Segre-
705 Cinca system). They are clearly associated to autumn fed when the snow cover
706 is generally absent and, more rarely, in spring. These are associated to long-
707 lasting rainfall (more than 10 days) and, also short but intense rainfall events (3

days) due to supply of warm and humid air from the Mediterranean Sea and enhanced convection by the orography.

c) Finally, the less common floods that affect only the lower course of the river, produced by high intensity thunderstorms (1 day). They have a fast and violent response (flash floods), but they have a reduced peak flow and a shorter time period compared to the previous floods.

Regarding the temporal evolution of the floods, we can distinguish two different periods. The first one, between 1600 and 1850, presents a low frequency of events, but includes probably the most important flood during the last millennia: October 1787, with a maximum specific discharge ratio among the largest ones in European rivers. The second period, since 1850, shows an increase in the frequency and magnitude of the events in the central Pyrenean basins and along the lower course. However, during the second part of the 20th century reservoirs play a fundamental role in regulating the peak flows throughout the whole system. This dynamic has also been observed in other basins in the IP and in the Mediterranean area, and it is related to an increase in climatic variability during the last stages of the Little Ice Age, to demographic changes and to reservoir constructions.

In all the studied cases, the maximum values of the reconstructed peak flows are higher than those recorded in the systematic series. This has important implications when calculating the return periods for these events, because the maximum peak flows for a given return period should be much higher than those calculated using only the systematic or instrumental series.

Acknowledgements

This work has been partially supported by the Spanish Ministry of Economy and Innovation (CGL2016-75996-R). A. Pelechá and J. Salleras, local historians in the town of Fraga, supplied valuable information about the historical floods of Fraga. O. Llanos helped in preparing in some of the figures. A. Abellà, D. Mérida, A. Monserrate, A. Sánchez and E. Thousaint helped with some of the numerical simulation models during their BSc. We would also like to acknowledge the data and support provided the Confederación Hidrográfica del Ebro.

739 **References**

740 Abadal, L.G., 1950. Una fecha trágica. La devastadora riada del 22 de octubre de 1907.
741 Ciudad, 2(10-11), pp. 152-153; pp. 168-170.
742 Abellà, A., 2013. Reconstrucció de les riuades més importants del riu Ebre al seu pas per
743 Móra d'Ebre. Master's Degree thesis. ETSEA, University of Lleida, 100 pp.
744 Albentosa, L.M., 1983. Precipitaciones excepcionales e inundaciones durante los días 6
745 al 8 de noviembre de 1982 en Cataluña. In: Albentosa, L.M. (ed.), Las lluvias
746 excepcionales en Cataluña en noviembre de 1982. Estudios Geográficos, 44:170/171,
747 pp. 229–273.
748 Andreassian V., 2004. Waters and forests: from historical controversy to scientific
749 debate. J. Hydrol. 291, 1–27.
750 Balasch, J.C., Remacha, R., Eritja, X., Sánchez, A., 2007. 1907 La riuada del Segre a Lleida.
751 Pagès Editors, Lleida, 229 pp.
752 Balasch, J.C., Ruiz-Bellet, J.L., Tuset, J., Martín de Oliva, J., 2010. Reconstruction of the
753 1874 Santa Tecla's rainstorm in western Catalonia (NE Spain) from flood marks and
754 historical accounts. Nat. Hazards Earth Syst. Sci. 10, 2317–2325.
755 Balasch, J.C., Ruiz-Bellet, J.L., Tuset, J., 2011. Historical flash floods retro modelling in the
756 Ondara River in Tàrrega (NE Iberian Peninsula). Nat. Hazards Earth Syst. Sci. 11, 3359-
757 3371.
758 Barrera-Escoda, A., Llasat, M.C., 2015. Evolving flood patterns in a Mediterranean region
759 (1301–2012) and climatic factors – the case of Catalonia. Hydrol. Earth Syst. Sci. 19, 465–
760 483.
761 Barriendos, M., 1997. Climatic variations in the Iberian Peninsula during the late
762 Maunder Minimum (AD 1675–1715): an analysis of data from rogation ceremonies.
763 Holocene 7 (1), 105–111. DOI: 10.1177/095968369700700110.
764 Barriendos, M., Martín Vide, J., 1998. Secular Climatic Oscillations as Indicated by
765 Catastrophic Floods in the Spanish Mediterranean Coastal Area (14th–19th Centuries),
766 Climatic Change 38, 473–491. DOI: 10.1023/a:1005343828552.
767 Barriendos, M., Llasat, M.C., 2003. The case of the 'Maldá' anomaly in the Western
768 Mediterranean Basin (AD 1760–1800): an example of a strong climatic variability.
769 Climatic Change 61 (1–2), 191–216.

770 Barriendos, M., Coeur, D., Lang, M., Llasat, M.C., Naulet, R., Lemaitre, F., Barrera, A.,
771 2003. Stationarity analysis of historical floods series in France and Spain (14th–20th
772 centuries). Nat. Hazards Earth Syst. Sci. 3, 583–592.
773 Barriendos, M., Rodrigo, F., 2006. Study of historical flood events on Spanish rivers using
774 documentary data. Hydrolog. Sci. J. 51 (5), 765–783.
775 Barriendos, M., Ruiz-Bellet, J.L., Tuset, J., Mazón, J., Balasch, J.C., Pino, D., Ayala, J.L.,
776 2014. The 'Prediflood' database of historical floods in Catalonia (NE Iberian Peninsula)
777 AD 1035–2013, and its potential applications in flood analysis, Hydrol. Earth Syst. Sci. 18,
778 1–17. DOI: 10.5194/hess-18-1-2014.
779 Batalla, R.J., Gómez, C.M., Kondolf, G.M., 2004. Reservoir-induced hydrological changes
780 in the Ebro River basin (NE Spain). J. Hydrol. 290, 117–136.
781 Batalla, R.J., Vericat, D., 2011. Hydrology and Sediment Transport. In D. Barceló and M.
782 Petrovic (eds): The Ebro River Basin. The Handbook of Environmental Chemistry, 13.
783 Springer, Berlín–Heidelberg, pp. 21–46.
784 Bayliss A.C., Reed, D.W., 2001. The use of historical data in flood frequency estimation.
785 Report to MAFF. CEH Wallingford, 87 p. Available at:
786 http://nora.nerc.ac.uk/8060/1/BaylissRepN008060CR.pdf, accessed: 15-05-2018.
787 Benito, G., Díez-Herrero, A., Fernández de Villalta, M., 2003. Magnitude and frequency
788 of flooding in the Tagus basin (central Spain) over the last millennium. Climatic Change
789 58, 171–192.
790 Benito, G., Lang, M., Barriendos, M., Llasat, M.C., Francés, F., Ouarda, T., Thorndycraft,
791 V.R., Enzel, Y., Bardossy, A., Coeur, D., Bobée, B., 2004. Use of systematic, paleoflood
792 and historical data for the improvement of flood risk estimation. Review of Scientific
793 Methods. Nat. Hazards 31, 623–643.
794 Benito, G., Ouarda, T.B.M.J., Bárdossy, A., 2005. Preface. Applications of paleoflood and
795 historical data in flood risk analysis. J. Hydrol. 313, 1–2.
796 Benito, G., Thorndycraft, V.R., Rico, M., Sanchez-Moya Y., Sopena, A., 2008. Palaeoflood
797 and floodplain records from Spain: evidence for long-term climate variability and
798 environmental changes. Geomorphology 101, 68–77.
799 Benito, G., Machado, M.J., 2012. Floods in the Iberian Peninsula. In Kundzewicz, Z.W.
800 (ed.): Changes in Flood Risk in Europe. IAHS Special Publication, 10, 2–12, Wallingford.

Benito, G. Brázdil, R., Herget, J., Machado, M.J., 2015a. Quantitative historical hydrology in Europe. Hydrol. Earth Syst. Sci. 19, 3517–3539.

Benito, G., Macklin, M., Cohen, K.M., Herget, J., 2015b. Past hydrological extreme events in a changing climate. Catena 130, 1–2.

Bladé, E., Cea, L., Corestein, G., Escolano, E., Puertas, J., Vázquez-Cendón, E., Dolz, J., Coll, A., 2012. Iber: herramienta de simulación numérica del flujo en ríos. Revista Internacional de Métodos Numéricos para Cálculo y Diseño en Ingeniería, 30 (1), 1–10.

Blasco-Ijazo, J., 1959. Las avenidas del Ebro. Crecidas verdaderamente extraordinarias 1261–1959. Librería General, Col. La Cadiera, n. 139, Zaragoza.

Blöschl, G., Montanari, A., 2010. Climate change impacts – throwing the dice? Hydrol. Process. 24, 374–381.

Boquera, M., 2008. Lo riu és vida: percepcions antropològiques de l'Ebre català. Tesi doctoral inèdita. Universitat Rovira i Virgili, Tarragona.

Brázdil, R., Kundzewicz, Z.W., 2006. Historical hydrology – Editorial. Hydrolog. Sci. J. 51 (5), 733–738.

Brázdil, R., Kundzewicz, Z.W., Benito, G., 2006. Historical hydrology for studying flood risk in Europe. Hydrolog. Sci. J. 51 (5), 739–764.

Brázdil, R., Kundzewicz, Z.W., Benito, G., Demarée, G., Macdonald, N., Roald, L.A., 2012. Historical floods in Europe in the past millennium. In Kundzewicz, Z.W. (ed.): Changes in Flood Risk in Europe. IAHS Special Publication, 10, 121–166, Wallingford.

Calder, I.R., Aylward, B., 2006. Forest and floods: Moving to an evidence-based approach to watershed and integrated flood management. Water Int. 31, 87–99.

Calenda, G., Mancini, C.P., Volpi, E., 2009. Selection of the probabilistic model of extreme floods: The case of the River Tiber in Rome. J. Hydrol., 371, 1–11.

Castelltort, X., Balasch, J.C., Ruiz-Bellet, J.L., Tuset, J., Barriendos, M., Mazon, J., Pino, D., 2015. Floods of the Segre River in Lleida (NE Iberian Peninsula) since 1500 AD. Geophysical Research Abstracts, vol. 17, EGU2015-2619-1, 2015 (https://presentations.copernicus.org/EGU2015-2619_presentation.pdf).

Catllar, B., Armengol, P., 1987. Atlas de Lleida. Segles XVII-XX. Col·legi d'Arquitectes de Catalunya, Demarcació de Lleida - La Paeria. Font Diestre, Hospitalet de Llobregat, 666 pp.

832 Corella, J.P., Benito, G., Rodríguez-Lloveras, X., Brauer, A., Valero-Garcés, B., 2014.
833 Annually-resolved lake record of extreme hydro-meteorological events since AD 1347 in
834 NE Iberian Peninsula. Quaternary Sci. Rev. 93, 77–90.
835 Corella, J.P., Valero-Garcés, B.L., Vicente-Serrano, S.M., Brauer, A., Benito, G., 2016.
836 Three millennia of heavy rainfalls in Western Mediterranean: frequency, seasonality and
837 atmospheric drivers. Sci. Rep. 6, 38206.
838 Curto, A., 2007. La riuada de 1907. La Riuada. Revista d'Informació Cultural (Móra
839 d'Ebre), 29, 4-8.
840 Davy, L., 1975. L'Ebre. Étude Hydrologique. PhD thesis. University Paul Valery,
841 Montpellier, 800 pp.
842 Del Valle, J., Ollero, A., Sánchez, M., 2007. Atlas de los ríos de Aragón. Ediciones Prames,
843 Zaragoza, 473 pp.
844 Elleder, L., 2010. Reconstruction of the 1784 flood hydrograph for the Vltava River in
845 Prague, Czech Republic. Global Planet. Change 70, 117–124.
846 Elleder, L., Herget, J., Roggenkamp, T., Nieben, A., 2013. Historic floods in the city of
847 Prague – reconstruction of peak discharges. Hydrolog. Res. 44, 202–214.
848 European Union 2007/60/EU.
849 Fernández, R., Lladonosa, M., 2003. Història de Lleida. 9 volumes, Pagès Editors, Lleida.
850 Fontseré, E., Galcerán, F., 1938. Les inundacions d'octubre del 1937 a l'Alt Pirineu.
851 Memòries (Servei Meteorològic de Catalunya), 1, 3, Generalitat de Catalunya, Barcelona,
852 15 pp.
853 Gallart, F., Llorens, P., 2004. Observation on land cover changes and water resources in
854 the headwaters of the Ebro catchment, Iberian Peninsula. Phys. Chem. Earth, 29(11–12),
855 769–773.
856 Galván, R., del Valle, J., Losada, J.A, Arnal, M., 2013. La inundación del Ebro de 1871 en
857 Zaragoza. Boletín de la Real Sociedad de Geografia 149, 139–169.
858 Galván, R., 2018. Cuatro grandes inundaciones históricas del Ebro en la ciudad de
859 Zaragoza: 1643, 1775, 1871, 1961. Papeles de Geografía 64. DOI:
860 10.6018/geografia/2018/302271.
861 García-Faria, P., 1908. Las inundaciones de octubre de 1907 en Catalunya. Revista de
862 Obras Públicas, I, 56. 1686: pp. 34-37, 1688: pp. 49-55, 1689: pp. 65-67, 1694: pp. 121-

125, 1696: pp. 148-150, 1698: pp. 175-176, 1703: pp. 236-238, 1704: pp. 248-249, 1705: pp. 258-260.

García-Ruiz, J.M., Lasanta, T., Martí, C., González, C., White, S., Ortigosa, L.M., Ruiz-Flaño, P., 1995. Changes in runoff and erosion as a consequence of land-use changes in the Central Spanish Pyrenees. Phys. Chem. Earth 20, 301–307.

Garcia, J., Payà, X., 1999. Excavacions a l'antic barri de Cappont i a la sèquia de Torres. Iltirda Lleida: Ajuntament de Lleida, Regidoria de Cultura.

Gaume, E., Livet, M., Desbordes, M., Villeneuve, J., 2004. Hydrological analysis of the river Aude, France, flash flood on 12 and 13 November 1999. J. Hydrol., 286, 135–154.

Glaser, R., Riemann, D., Schönbein, J., Barriendos, M, Brázdil, R., Bertolin, C., Camuffo, D., Deutsch, M., Dobrovolný, P., van Engelen, A., Enzi, S., Halíèková, M., Koenig, S.J., Kotyza, O., Limanówka, D., Macková, J., Sghedoni, M., Martin, B., Himmelsbach, I., 2010. The variability of European floods since AD 1500. Climatic Change 101, 235–256.

González-Sampériz, P., Aranbarri, J., Pérez-Sanz, A., Gil-Romera, G., Moreno, A., Leunda, M., Sevilla-Callejo, M., Corella, J.P., Morellón, M., Oliva, B., Valero-Garcés, B., 2017. Environmental and climate change in the southern Central Pyrenees since the Last Glacial Maximum: A view from the lake records. Catena 149, 668–688.

Gregory, K.G., Benito, G., Dikau, R., Golosov, V., Jones, A.J.J., Macklin, M.G., Parsons, A.J., Passmore, D.G., Poesen, J., Starkel, L., Walling, D.E., 2006. Past hydrological events related to understanding global change: An ICSU research project. Catena 66, 2–13.

Hall, J., Arheimer, B., Borga, M., Brázdil, R., Claps, P., Kiss, A., Kjeldsen, T. R., Kriaučiūnienė, J., Kundzewicz, Z. W., Lang, M., Llasat, M. C., Macdonald, N., McIntyre, N., Mediero, L., Merz, B., Merz, R., Molnar, P., Montanari, A., Neuhold, C., Parajka, J., Perdigão, R. A. P., Plavcová, L., Rogger, M., Salinas, J. L., Sauquet, E., Schär, C., Szolgay, J., Viglione, A., Blöschl, G., 2014. Understanding flood regime changes in Europe: a state-of-the-art assessment, Hydrol. Earth Syst. Sci. 18, 2735–2772.

Herget, J., Meurs, H., 2010. Reconstructing peak discharges for historic flood levels in the city of Cologne – Germany. Global Planet. Change 70, 108–116.

Herget, J., Roggenkamp, T., Krell, M., 2014. Estimation of peak flood discharges of historical floods. Hydrol. Earth Syst. Sci. 11, 5463–5485.

Herschy, R., 2003. World Catalogue of Maximum Observed Floods. IAHS Publ. 284, Wallingford (UK), 285 pp.

895 Iglesies, J., 1971. L'aiguat de Santa Tecla (23 de setembre de 1874). Episodis de la
896 Història, 156. R. Dalmau, Barcelona, 62 pp.
897 IPCC, 2003. Summary for policymakers. In: Stocker, T.F., Qin, D., Plattner, G.K., Tignor,
898 M., Allen, S.K., Boschung, J., Nauels, A., Xia, Y., Bex, M., Midgley, P.M. (eds.): Climate
899 Change 2013: The Physical Science Basis, Contribution of Working Group I to the Fifth
900 Assessment Report of the Intergovernmental Panel on Climate Change. Cambridge
901 University Press, Cambridge (UK) and New York (USA).
902 Kjeldsen, T.R., Macdonald, N., Lang, M., Mediero, L., Albuquerque, T., Bogdanowicz, E.,
903 Brázdil, R., Castellarin, A., David, V., Fleig, A., Gül, G.O., Kriauciuniene, J., Kohnová, S.,
904 Nicholson, O., Roald, L.A., Salinas, J.L., Sarauskiene, D., Sraj, M., Strupczewski, W.,
905 Szolgay, J., Toumazis, A., Vanneuville, W., Veijalainen, N., Wilson, D., 2014. Documentary
906 evidence of past floods in Europe and their utility in flood frequency estimation. J.
907 Hydrol. 517, 963–973.
908 Knox, J. C., 2000. Sensitivity of modern and Holocene floods to climate change,
909 Quaternary Sci. Rev. 19, 439–457.
910 Kundzewicz Z.W., Kanae, S., Seneviratne, S.I., Handmer, H., Nicholls, N., Peduzzi, P.,
911 Mechler, R, Bouwer, L.M., Arnell, N., Mach, K., Muir-Wood, R., Brakenridge, G.R., Kron,
912 W., Benito, G., Honda, Y., Takahashi, K., Sherstyukov, B., 2014. Flood risk and climate
913 change: global and regional perspectives. Hydrol. Sci. J. 59 (1), 1–28.
914 Lang, M., Fernández-Bono, J.F., Recking, A., Naulet, R., Grau-Gimeno, P., 2004.
915 Methodological guide for palaeoflood and historical peak discharge estimation. In
916 Benito, G., Thorndycraft, V.R. (eds.): Systematic, Palaeoflood and Historical Data for the
917 Improvement of Flood Risk Estimation: Methodological Guidelines. CSIC – Centro de
918 Ciencias Mediambientales, Madrid, 43–53.
919 Lladonosa, J., 1975. Historia de Lleida. Vol. 2. F. Camps Calmet Editor, Tàrrega, 907 pp.
920 Llasat, M.C., Barriendos, M., Barrera, A., Rigo, T., 2005. Floods in Catalonia (NE Spain)
921 since the 14th century. Climatological and meteorological aspects from historical
922 documentary sources and old instrumental records. J. Hydrol. 313, 32–47.
923 Llop, C., 1995. Atlas urbanístic de Lleida 1707-1995. Ajuntament de Lleida-Col·legi
924 d'Arquitectes de Catalunya, Demarcació de Lleida. 133 pp.
925 López-Bustos, A., 1972. Antecedentes para una historia de avenidas del río Ebro. Revista
926 de Obras Públicas, 3083, 191–204.

López-Bustos, A., 1981. Tomando el pulso a las grandes crecidas de los ríos peninsulares. Revista de Obras Públicas, 3190, 179–192.

López-Moreno, J.I., Vicente-Serrano, S.M., Zabalza, J., Beguería, S., Lorenzo-Lacruz, J., Azorín-Molina, C., Morán-Tejeda, E., 2013. Hydrological response to climate variability at different time scales: A study in the Ebro basin. J. Hydrol. 477, 175–188.

Luterbacher, J., García-Herrera, R., Akcer-On, S., Allan, R., Alvarez-Castro, M.C., Benito, G., Booth, J., Büntgen, U., Cagatay, N., Colombaroli, D., Davis, B., Esper, J., Felis, T., Fleitmann, D., Frank, D., Gallego, D., Garcia-Bustamante, E., Glaser, R., González-Rouco, J.F., Goosse, H., Kiefer, T., Macklin, M. G., Manning, S.W., Montagna, P., Newman, L., Power, M. J., Rath, V., Ribera, P., Riemann, D., Roberts, N., Sicre, M., Silenzi, S., Tinner, W., Valero-Garces, B., van der Schrier, G., Tzedakis, C., Vannière, B., Vogt, S., Wanner, H., Werner, J. P., Willett, G., Williams, M.H., Xoplaki, E., Zerefos, C.S. Zorita, E., 2012. A review of 2000 years of paleoclimatic evidence in the Mediterranean. In: Lionello, P. (ed.), The Climate of the Mediterranean region: from the past to the future. Elsevier, Amsterdam, The Netherlands, 87–185.

Macdonald, N., Sangster, H., 2017. High-magnitude flooding across Britain since AD 1750. Hydrol. Earth Syst. Sci. 21, 1631–1650.

Machado, M.J., Benito, G., Barriendos, M., Rodrigo, F.S., 2011. 500 years of rainfall variability and extreme hydrological events in southeastern Spain drylands. J. Arid Environ. 75, 1244–1253.

Machado, M.J., Botero, B.A., López, J, Francés, F., Díez-Herrero, A., Benito, G., 2015. Flood frequency analysis of historical flood data under stationary and non-stationary modelling. Hydrol. Earth Syst. Sci. 19, 2561–2576.

Macklin, M.G., Benito, G., Gregory, K.J., Johnstone, E, Lewin, J., Michczyñska, D.J., Soja, R., Starkel, L., Thorndycraft, V.R., 2006. Past hydrological events reflected in the Holocene fluvial record of Europe. Catena 66, 145–154.

Magdaleno, F., Fernández-Yuste, J.A., 2011. Meander dynamics in a changing river corridor. Geomorphology 130, 197–207.

Marcuello, J.R., 2001. El Ebro, tierras y gentes. El Periódico de Aragón, Zaragoza, 320 pp.

Merz, B., Aerts, J., Arnbjerg-Nielsen,K., Baldi, M., Becker, A., Bichet, A., Blöschl, G., Bouwer, L.M., Brauer, A., Cioffi, F., Delgado, J.M., Gocht, M., Guzzetti, F., Harrigan, S., Hirschboeck, K., Kilsby, C., Kron, W., Kwon, H.-H., Lall, U., Merz, R., Nissen, K., Salvatti,

959 P., Swierczynski, T., Ulbrich, U., Viglione, A., Ward, P.J., Weiler, M., Wilhelm, B., Nied,
960 M., 2014. Floods and climate: emerging perspectives for flood risk assessment and
961 management. Nat. Hazards Earth Syst. Sci. 14, 1921–1942.
962 Milly, P.C.D., Betancourt, J., Falkenmark, M, Hirsch, R.M., Kundzewicz, Z.W.,
963 Lettenmaier, D.P., Stouffer, R.J., 2008. Stationarity is dead: whither water management?
964 Science 319, 573–574.
965 Miravall, R., 1997a. La tragèdia de les riuades de l'Ebre. La Riuada. Revista d'Informació
966 Cultural (Móra d'Ebre), 9, 4–6.
967 Miravall, R., 1997b. Flagells naturals sobre Tortosa. Ed. Columna-Tresmall.
968 Monserrate, A., 2013. Reconstrucción de las avenidas de finales del siglo XIX en
969 Zaragoza. Master's Degree thesis. ETSEA, University of Lleida, 79 pp.
970 Naulet, R., Lang, M., Ouarda, T.B.M.J., Coeur, D., Bobée, B., Recking, A., Moussay, D.,
971 2005. Flood frequency analysis on the Ardèche river using French documentary sources
972 from the last two centuries. J. Hydrol. 313, 58–78.
973 Oliva, M., Ruiz-Fernández, J., Barriendos, M. Benito, G., Cuadrat, J.M. Domínguez-Castro,
974 F., J.M. García-Ruiz, J.M., S. Giralt, S., Gómez-Ortiz, A., Hernández, A., López-Costas, O.,
975 López-Moreno, J.I., López-Sáez, J.A., Martínez-Cortizas A., Moreno,A., Prohom, M, Saz,
976 M.A., Serrano, E., Tejedor, E., Trigo, R., Valero-Garcés, B., Vicente-Serrano, S.M., 2018.
977 The Little Ice Age in Iberian mountains. Earth-Sci. Rev. 177, 175–208.
978 Ollero, A., 2010. Channel changes and floodplain management in the meandering
979 middle Ebro River, Spain. Geomorphology 117, 247–260.
980 Ollero, A., Sánchez, M., Losada, J.A., Hernández, C., 2004. El comportamiento hídrico del
981 río Ebro en su recorrido por Aragón. In Peña, J.L., Longares, L.A., Sánchez, M. (eds.):
982 Geografía Física de Aragón. Aspectos generales y temáticos. Universidad de Zaragoza-
983 Institución Fernando el Católico, Zaragoza, 243–252.
984 Peña, J.C., Pino, D., Balasch, J.C., Prohom, M., Barriendos, M., Ruiz-Bellet, J.L., Tuset, J.,
985 Mazon, J., Schulte, L., 2017. Synoptic aspects of large floods in the south of Catalonia
986 (Spain). EMS Annual Meeting. 4–8 September, Dublin, Ireland.
987 Pino, D., Ruiz-Bellet, J. L., Balasch, J. C., Romero-León, L., Tuset, J., Barriendos, M.,
988 Mazon, J., Castelltort, X., 2016. Meteorological and hydrological analysis of major floods
989 in NE Iberian Peninsula. J. Hydrol. 541, 63–89.

990 Pleyán de Porta, J., 1945. Efemérides leridanas recogidas y ordenadas. Institut d'Estudis
991 Ilerdencs, Lleida, Spain.
992 Prohom, M., Barriendos, M., Sánchez-Lorenzo, A., 2016. Reconstruction and
993 homogenization of the longest instrumental precipitation series in the Iberian Peninsula
994 (Barcelona, 1786–2014). Int. J. Climatol. 36(8), 3072–3087.
995 Querol, E., 2006. Les riuades de l'Ebre a la literatura. Recerca, 10, 261–300.
996 Remo, J.W.F., Pinter, N., 2007. Retro-modeling the Middle Mississippi River. J. Hydrol.
997 337, 421–435.
998 Roggenkamp, T., Herget, J., 2014. Reconstructing peak discharges of historic floods of
999 the River Ahr – Germany. Erdkunde 68, 49–59.
1000 Ruiz-Bellet, J.L., Balasch, J.C., Tuset, J., Barriendos, M., Mazon, D., Pino, D., 2015a.
1001 Historical, hydraulic, hydrological and meteorological reconstruction of 1874 Santa Tecla
1002 floods in Catalonia (NE Iberian Peninsula). J. Hydrol. 524, 279–295.
1003 Ruiz-Bellet, J.L., Balasch, J.C., Tuset, J., Monserrate, A., Sánchez, A., 2015b. Improvement
1004 of flood frequency analysis with historical information in different types of catchments
1005 and data series within the Ebro River basin (NE Iberian Peninsula). Z. Geomorphol., 59
1006 Suppl. 3 127–157.
1007 Ruiz-Bellet, J.L., Castelltort, X., Balasch, J.C., Tuset, J., 2017. Uncertainty of the peak flow
1008 reconstruction of the 1907 flood in the Ebro River in Xerta (NE Iberian Peninsula). J.
1009 Hydrol. 545, 339–354.
1010 Salleras, J., Espinosa, R., 1994. Fraga y el Cinca: Sus puentes y barcas. Amics de Fraga,
1011 Fraga, 330 pp.
1012 Sánchez, A., 2007. Modelización hidráulica y análisis de magnitud-frecuencia de
1013 avenidas históricas en el curso bajo del río Ebro. Master's Degree thesis. ETSEA,
1014 University of Lleida, 41 pp.
1015 Sheffer, N.A., Rico, M., Enzel, Y., Benito, G., Grodek, T., 2008. The paleoflood record of
1016 the Gardon river, France: a comparison with the extreme 2002 flood event.
1017 Geomorphology 98, 71–83.
1018 Stanescu, V.A., 2004. Le potentiel des grandes crues de l'Europe, leurs regionalisation et
1019 comparaison. La Houille Blanche, 6, 21–27.

1020 Thorndycraft, V.R., Barriendos, M., Benito, G., Rico, M., Casas, A., 2006. The catastrophic
1021 floods of AD 1617 in Catalonia (northeast Spain) and their climatic context. Hydrolog.
1022 Sci. J. 51 (5), 899–912.
1023 U.S. Army Corps of Engineers (USACE)(2010a. HEC-GeoRAS GIS Tools for Support of HEC-
1024 RAS using ArcGIS. User's Manual. Version 4.3.93. U.S. Army Corps of engineers
1025 Hydrologic Engineering Center, Davis, California.
1026 U.S. Army Corps of Engineers (USACE), 2010b. HEC-RAS River Analysis System: User's
1027 Manual. Version 4.1. U.S. Army Corps of Engineers, Hydrologic Engineering Center,
1028 Davis, California.
1029 Vicente-Serrano, S.M.; López-Moreno, J.I., Beguería, S., 2007. La precipitación en el
1030 Pirineo español: Diversidad espacial en las tendencias y escenarios futuros. Pirineos
1031 162, 43–69.

1032 **TABLES**

1033 **Table 1.** Morphological, climatic and mean hydrological characteristics of the four
1034 analyzed subbasins.

Subbasin	Area		Contribution to runoff (%)	River length (km)	Mean channel slope (mkm^{-1})	Predominant climates	Hydrological regime
	Size (km^2)	Percentage over total Ebro area (%)					
Upper Ebro	40434	47%	54%	588	2.8	Atlantic/Continental/Subalpine	Pluvio-nival
Cinca	9699	11%	18%	170	12.5	Alpine/Mediterranean/Semiarid	Nivo-pluvial
Segre	12880	15%	19%	265	8.7	Alpine/Mediterranean/Semiarid	Pluvio-nival
Lower Ebro	21998	25%	9%	342	0.46	Mediterranean/Semiarid	Pluvial
Ebro at the mouth	85362	100%	100%	930	---	---	Pluvio-nival

1035

1036 **Table 2.** Measured mean and maximum peak flows at the four analyzed sites.

Subbasin	Site	Distance to Tortosa (km)	Gauging record starting year	Measured flow				
				Mean flow (m^3s^{-1})	Specific mean flow ($m^3s^{-1}km^{-2}$)	Maximum peak flow (m^3s^{-1}) and year of occurrence	Maximum specific peak flow ($m^3s^{-1}km^{-2}$)	Maximum peak flow / mean flow
Upper Ebro	Zaragoza	342	1913	231	0.006	4130 (1961)	0.10	18
Cinca	Fraga	133	1928	78	0.008	4200 (1982)	0.43	54
Segre	Lleida	153	1913	80	0.006	3600 (1937)	0.28	45
Whole Ebro	Tortosa	0	1913	428	0.005	9250 (1937)	0.11	22

1037
1038

1039 **Table 3.** Sources of information.
1040

Site	Meteorological, hydrological and hydraulic information			Channel geometry information
	Consulted archives and institutions	**Flood lists, flood descriptions**	**Peak hydraulic modeling**	**Old city maps, etchings, drawings, paintings**
Zaragoza	- Zaragoza Urbanistic Archives - Archives of the Confederación Hidrográfica del Ebro (CHE) in Zaragoza	Blasco-Ijazo (1959) Galván (2018) Galván et al. (2013) Marcuello (2001)	Monserrate (2013) Ruiz-Bellet et al. (2015b)	Painting by J. Bautista Martínez del Mazo (1647) Map by Rapins-Tindals (1710) Anonymous engraving (1820) City map by Casañal (1879) Puente de Piedra (1972) elevation blueprint (1972, CHE Archives)
Fraga	- Town Hall Archive - Regional Archive of the Palau de Montcada - Archives of the Corona d'Aragó in Barcelona	Salleras and Espinosa (1994)	No previous information	Baldi's engraving (1668) Anonymous (1779) Anonymous (1799) Anonymous (1885)
Lleida	- Book of Minutes of the Municipal Council (Paeria House) - Municipal Archive of Lleida - Chapterhouse Archives of the Lleida Cathedral	Fernández and Lladonosa (2003) Lladonosa (1975) Pleyán de Porta, (1945)	Balasch et al. (2007) Castelltort et al. (2015)	Atlas of old city maps of Catllar and Armengol (1987) Atlas of old city maps of Llop (1995)
Tortosa	- Chapterhouse Archives of the Tortosa Cathedral - Historical Municipal Archives of Tortosa - Ebro Observatory in Roquetes	Boquera (2008) Curto (2007) Miravall (1997a) Querol (2006)	Ruiz-Bellet et al. (2015b) Ruiz-Bellet et al. (2017) Sánchez (2007)	Wyngaerde's engraving (1563) Sier de Beaulieu's engraving (1648) V. der Aa's engraving (1707) Map of Collin (1811)

1041

1042

1043 **Table 4.** Parameters used in the hydraulic modeling of the reconstructed peak flows.
1044

Site	Software	Reach length (m)	Number of cross sections	Mean slope (mkm^{-1})	Manning coefficient (channel/banks/forest/ floodplain)
Zaragoza	HEC-RAS v.4.1.0	10500	142 (5m×5m)	0.5	channel: 0.0023 orchards: 0.037 urban areas: 0.127 riparian dense forest: 0.1 riparian sparse forest: 0.06 wasteland: 0.03
Fraga	IBER 2-D v.2.4	6000	(10m×10m)	2.1	Mean weighted coefficient: 0.05
Lleida	HEC-RAS v.4.1.0 and IBER 2-D v.2.4	7750	18 (10m×10m)	1.6	channel:0.035 banks: 0.04 riparian forest and urban areas: 0.1 floodplain: 0.04
Tortosa	HEC-RAS v.4.1.0 and IBER 2-D v.2.4	7690	45 (5m×5m)	0.24	channel: 0.039 riparian dense forest: 0.1 dense scrubland: 0.1 orchards: 0.06 urban areas: 0.03

1045

Table 5. Main floods in the Ebro River section at Zaragoza since the 17th century. Dates in bold indicate the largest floods (Q>3500 m^3s^{-1}).

Date of peak flow at Zaragoza	Reference site[a,b] or source	Height over the riverbed (m)	Height (m a.s.l.)	Reliability[c]	Precision[d] (cm)	Maximum peak discharge (m^3s^{-1})
18-2-1643	Predicadores (Preachers) Monastery: 0.83 m over the walls	9.33[e]	199.33	2	25	5560
25-6-1775	Water enters Sancho's gate	8.95[f]	198.95	2	25	5180
9-10-1787	Almost reaches Sancho's gate	8.45[f]	198.45	2	25	4600
13-1-1871	Stone bridge (iron ring)	6.7[g]	195.93	3	10	4844
Jan-1874	Stone bridge (iron ring)	5.92[g]	195.15	3	10	3624
1878	Stone bridge (iron ring)	5.36[g]	194.59	3	10	2805
1888	Stone bridge (iron ring)	4.61[g]	193.84	3	10	1965
18-11-1906	López-Bustos (1972)	5.58	194.81			3030
23-10-1907	López-Bustos (1972)	4.34	193.57			1700
17-3-1930	CHE database	5.89	195.12			3600
29-10-1937	CHE database	5.57	194.8			3020
2-1-1961	CHE database, calibration stone bridge	6.32	195.55	3	10	4130
9-11-1982	CHE database	4.6	193.83			1910

[a] For the Sancho's gate and Preachers Monastery references, every ±25 cm of difference in the section located at Sancho's gate is equivalent to a difference of ±250 m^3s^{-1} in the maximum peak discharge.

[b] From 1871 until 1961 (scale at the Stone Bridge), we assume for the reconstructions that a variation of ±10 cm of the water height is equivalent to ±200 m^3s^{-1}.

[c] According to the definition by Bayliss and Reed (2001): 1-unreliable, 2-reliable, 3-very reliable.

[d] Expected maximum difference (cm) between the observed and simulated maximum water mark.

[e] Level refers to the section at the Preachers Monastery.

[f] Level refers to the section at the Sancho's Gate.

[g] Level refers to the scale installed by the CHE at the Stone Bridge up the end of the 1960's and can be observed on a map on 1972. The current scale was moved in the 1970's to the Santiago Bridge.

1063 **Table 6.** Main floods in the Cinca river section at Fraga since 17th century. Dates in bold
1064 indicate the most important floods (Q≥2500 m^3s^{-1}).

Date of the peak flow at Fraga	Reference site or source	Height over the riverbed (m)	Height (m a.s.l.)	Reliability[a]	Precision[b] (cm)	Maximum peak discharge (m^3s^{-1})
25-12-1607	Damages at the bridge[f]					
8-11-1617	A royal traveler explains the bridge is broken			1		2500[c]
6-5-1762	Destroys the bridge[f]					
10-10-1787	It affects the Capuchin Monastery[e]			1		2500[c]
6-9-1788	Water is 1.5 m at the Capuchin Monastery[f]	6.02	99.49	2	50	4500[d]
28-9-1852	Destroys a suspended bridge[f]					
24-05-1853	Water reaches the fort and a small bridge at the Capuchin Monastery [f]			1		3000[c]
21-10-1866	The second suspended bridge disappears[f]			1		3000[c]
1882	Destroys the bridge, 40 people drown[f]					
23-9-1874	Affects the bridge without destroying any pillars[f]			1		2500[c]
23-10-1907		5.35	98.82	3	10	3900[e]
29-10-1937				3	10	2600[e]
9-11-1982		5.76	99.23	3	10	4200[e]

1065 [a] According to the definition by Bayliss and Reed (2001): 1-unreliable, 2-reliable, 3-very
1066 reliable.

1067 [b] Expected maximum difference (cm) between the observed and simulated maximum
1068 water marks.

1069 [c] Estimated from the hydraulic budget between subbasins.

1070 [d] Modeled with HEC-RAS by using an approximated flow mark.

1071 [e] Calculated by the CHE.

[f] Salleras and Espinosa (1994).

1073 **Table 7.** Main floods in the Segre River section at Lleida since the 17th century. Dates in
1074 bold indicate the largest floods (Q>3000 m^3s^{-1}).

Date of the peak flow at Lleida	Reference site or source	Height over the riverbed (m)	Height (m a.s.l.)	Reliability[a]	Precision[b] (cm)	Maximum peak discharge (m^3s^{-1})
1604	Flood at the Trinity and Saint Agustin Monasteries (Garcia and Payà, 1999)	7	146.5	2	50	3000
8-11-1617	The Blessed Sacrament of the Saint Agustin Monastery was saved by boat (Lladonosa, 1975)	8	147.5	2	50	4000
11-10-1625	Flood at Cappont	7	146.5	2	50	3000
1726	3 pillars destroyed Some houses by the river are evacuated	8.5	148.0	2	50	
17-12-1766	The water reaches the Trinity Monastery	7.5	147.0	2	50	3500
14-06-1773	The water reaches beyond the Trinity Monastery	7	146.5	2	50	
8-10-1787	Façade of the gate of Arc del Pont	12.3	151.8	2	20	8500
6-1-1826	Flood over the orchards	6.5	146.0	2	50	
24-05-1853	Water reaches the second step of the stairs of the new Cathedral*. Rambla de Ferran** (2 m)	9.3	146.5* 148.8**	3	20	6000
21-10-1866	Lower than the previous flood, but it destroys two arcs of the bridge	8.3	147.8	3	50-100	5000
23-9-1874	Floods Rambla de Ferran, 1 m below the level of the 1853 flood (Iglesies, 1971)	7.5	147	3	50	3200
23-10-1907	Flood reaches Rambla de Ferran* (García-Faria, 1908) and the first step of the stairs of the new Cathedral** (Abadal, 1950) Pillar of the Theater Camps Elisis***	9.1	148.6* 146.2** 147.8***	3	20-30	5250
29-10-1937	Water enters into Rambla de Ferran	7.7	147.2	3	20	3600

9-11-1982	Water enters into Rambla de Ferran 1.5 m of water at the Civil Government building	8.5	148	3	10	3400

[a] According to the definition by Bayliss and Reed (2001): 1-unreliable, 2-reliable, 3-very reliable.

[b] Expected maximum difference (cm) between the observed and simulated maximum water marks.

1080 **Table 8.** Main floods in the Ebro River section at Xerta (Sant Martí church) since the 17th
1081 century. Dates in bold indicate the largest floods (Q>4500 m^3s^{-1}).

Date of the peak flow at Tortosa	Reference site or source	Height over the riverbed (m)	Height (m a.s.l.)	Reliability[a]	Precision[b] (cm)	Maximum peak discharge (m^3s^{-1})
5-11-1617	Xerta scale	7.66	13.83	3	10	7500
9-10-1787	Xerta scale	9.98	16.15	3	10	12900
25-5-1853	Xerta scale	8.06	14.23	3	10	8250
21-10-1866	Xerta scale	7.86	14.03	3	10	7750
21-1-1871	Xerta scale	6.41	12.58	3	10	5000
17-9-1884	Xerta scale	7.24	13.41	3	10	6500
23-10-1907	Xerta scale	9	15.17	3	10	10500
29-10-1937	Xerta scale	8.50	14.67	3	10	9250
4-1-1961	Xerta scale	6	12.17	3	10	4580
9-11-1982	Scale Tortosa (CHE)					3780

1082 [a] According to the definition by Bayliss and Reed (2001): 1-unreliable, 2-reliable, 3-very
1083 reliable.

1084 [b] Expected maximum difference (cm) between the observed and simulated maximum
1085 water mark.

Table 9. Maximum peak discharges of the 16 analyzed floods in the four subbasins and their respective contributions to the total peak discharge at Tortosa.

Date of the peak flow at Tortosa			Peak flow (m^3s^{-1})				Most contributing subbasin
Day	Month	Year	Upper Ebro at Zaragoza	Cinca at Fraga	Segre at Lleida	Ebro at Tortosa	
8	11	1617	NF	2500[a]	4000[b]	7500[c]	Cinca+Segre
18	2	1643	5560[b]	NF	NF	< 4500[c]	Upper Ebro
19	12	1766	NF	NF	3500[b]	< 4500[c]	Segre
25	6	1775	5180[b]	NF	NF	< 4500[c]	Upper Ebro
9	10	1787	4600[b]	2500[a]	8500[b]	12900[c]	Upper Ebro+Cinca+Segre
25	5	1853	NF	3000[a]	6000[c]	8250[c]	Cinca+Segre
21	10	1866	NF	3000[a]	5000[b]	7750[c]	Cinca+Segre
13	1	1871	4844[c]	NF	NF	5000[c]	Upper Ebro
---	1	1874	3624[c]	NF	NF	< 4500[c]	Upper Ebro
23	9	1874	NF	2500[a]	3200[b]	< 4500[c]	Cinca+Segre+Lower Ebro
17	9	1884	NF	NF	NF	6500[c]	Lower Ebro
23	10	1907	1700[d,f]	3900[d]	5250[c]	10500[c]	Upper Ebro+Cinca+Segre
17	03	1930	3600[e]	NF	NF	3000[e]	Upper Ebro
29	10	1937	3020[e]	2600[d]	3600[d,g]	9250[c]	Upper Ebro+Cinca+Segre
2	1	1961	4130[e]	NF	NF	4580[e]	Upper Ebro
9	11	1982	1910[e]	4200[e]	3400[e]	3780[e]	Cinca+Segre

NF = no flood.

[a] Estimated by performing an hydraulic budget between subbasins.

[b] Modeled with HEC-RAS or IBER from an approximate flood mark.

[c] Modeled with HEC-RAS or IBER from an exact flood mark.

[d] Calculated by López-Bustos (1972).

[e] Calculated by the Confederación Hidrográfica del Ebro (CHE) or the Centro de Estudios y Experimentación de Obras Públicas (CEDEX) (Spanish Hydraulic Administrations).

[f] 1200 m^3s^{-1} need to be added to this value due to the contribution of the Gállego River, downstream Zaragoza.

[g] Compilated by Fontseré and Galcerán (1938).

1098 **Table 10.** For each analyzed flood, information about the influence of antecedent precipitation, floods and snowmelt.

Date of peak flow at Tortosa			Number of cases with torrential or persistent rain or floods registered in the AMICME database[a] for each subbasin of the Ebro basin during the 15 days before the event				Number of cases with torrential or persistent rain or floods in the AMICME database[a] in adjacent basins during the 15 days before the event		Snowmelt information in the AMICME database[a] or in other sources	Observations
Day	Month	Year	Upper Ebro	Cinca	Segre	Lower Ebro	Northeast of the Ebro basin[b]	Southeast of the Ebro basin[c]		
8	11	1617		1	7		7	2	Without data	30 days of rainfall during Oct. and beginning of Nov.[d]
18	2	1643				1			Yes	Snow in Catalonia. Cold winter
19	12	1766			2	1	4		Yes	Continuous rainfall since mid Sept. Failed harvests
25	6	1775	1					1	No[e]	Flood in Bilbao (Nervión River) on 20 June
9	10	1787	9		7	1	4	7	No	More than 10 days of rainfall and thunderstorms. There is a previous flood of the Aragón River 14 days before
25	5	1853	2	1	7		8		Yes	Rainy May (238 mm in Barcelona) and torrential rainfall during the 3 days before the event[a]
21	10	1866				4	8	1	No	Two rainfall periods of 5 days separated by 14 days. 330 mm over the last 30 days in Barcelona[a]

13	1	1871	2				1		Yes	Snow precipitations in Dec. and Jan. Three rainfall days before the event[f]
---	1	1874	1						Without data	
23	9	1874		1	2	4			No	155 mm/6h[g]
17	9	1884		1		4	3	3	No	Estimated runoff volume: 560 hm^3 [h]
23	10	1907		1	13		30		No	During Oct., 217 mm accumulated until 23rd in Puigcerdà (headwaters of Segre River)[i] 200-360 mm of rain in the central Pyrenees during the last 3 days[j] Estimated runoff volume: 3000 hm^3 [h]
17	03	1930					2		Yes	50-60 cm of snow in the Pyrenees 12-13 Jan. 3 rainy days and strong snowmelt[j]
29	10	1937			2				No	300-430 mm of rain in the central Pyrenees over 3 days[k]
2	1	1961	1						Yes	62 cm of snow in the central Pyrenees in Dec. 1960. Very wet winter in Central and Western Pyrenees[l] Estimated runoff volume: 4000 hm^3 [h]
9	11	1982					4	2	No	240-640 mm of rain in the central Pyrenees over 3 days[m] Estimated runoff volume: 925 hm^3 [h]

[a]Barriendos et al. (2014).
[b]Llobregat, Ter, Besos, and Francolí river basins.
[c]Turia, Jucar, and Segura river basins.
[d]Thorndycraft et al. (2006).
[e]Galván (2018).
[f]Galván et al. (2013).
[g]Estimated by Ruiz-Bellet et al. (2015a).
[h]CEDEX.

[i]Balasch et al. (2007).
[j]Marcuello (2001).
[k]Fontseré and Galcerán (1938).
[l]Marcuello (2001).
[m]Albentosa (1983).

Table 11. List of the main floods in the Ebro basin since 1617, and their occurrence in to the four studied sites. Colors indicate the flood-generating process (see legend below).

Ebro NW → SE				Cinca	Segre
Miranda	Logroño	Zaragoza	Tortosa	Fraga	Lleida
---	---	---	1617 (Nov)	1617 (Nov)	1617 (Nov)
---	---	1643 (Feb)	---	---	---
---	---	---	1766 (Dec)	---	1766 (Dec)
1775 (June)	1775 (June)	1775 (June)	---	---	---
---	---	1787 (Oct)	1787 (Oct)	1787 (Oct)	1787 (Oct)
1853 (May)	---	---	1853 (May)	1853 (May)	1853 (May)
---	---	---	1866 (Oct)	1866 (Oct)	1866 (Oct)
---	1871 (Jan)	1871 (Jan)	1871 (Jan)	---	---
1874 (Jan)	1874 (Jan)	1874 (Jan)	---	---	---
---	---	---	1874 (Sep)	1874 (Sep)	1874 (Sep)
---	---	---	1884 (Sep)	---	---
---	---	1907 (Oct)	1907 (Oct)	1907 (Oct)	1907 (Oct)
1930 (Mar)	1930 (Mar)	1930 (Mar)	---	---	---
---	---	1937 (Oct)	1937 (Oct)	1937 (Oct)	1937 (Oct)
1961 (Jan)	1961 (Jan)	1961 (Jan)	1961 (Jan)	---	---
---	---	---	1982 (Nov)	1982 (Nov)	1982 (Nov)

10 or more days of rain
Less than 10 days of rain
Snow melt + rain
Local flash flood
Flood-generating process not ascertained

FIGURES

Figure 1. a) Location of the Ebro basin within SE Europe and the Iberian Peninsula, and b) map of the Ebro River basin and subbasins, with the most important sites, reservoirs and canyons located along the lower course.

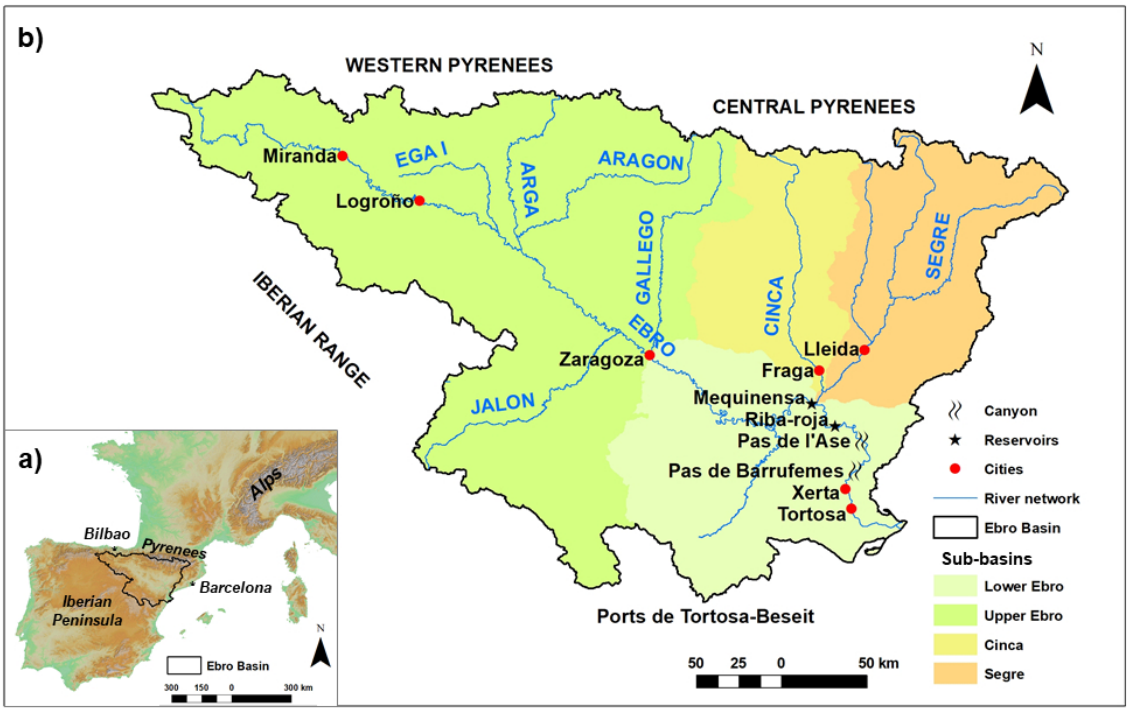

Figure 2. Maximum annual discharge (Qci) by month for the Ebro at Zaragoza, the Cinca at Fraga, the Segre at Lleida, and the Ebro at Tortosa. The number of Qci values for each site are also indicated.

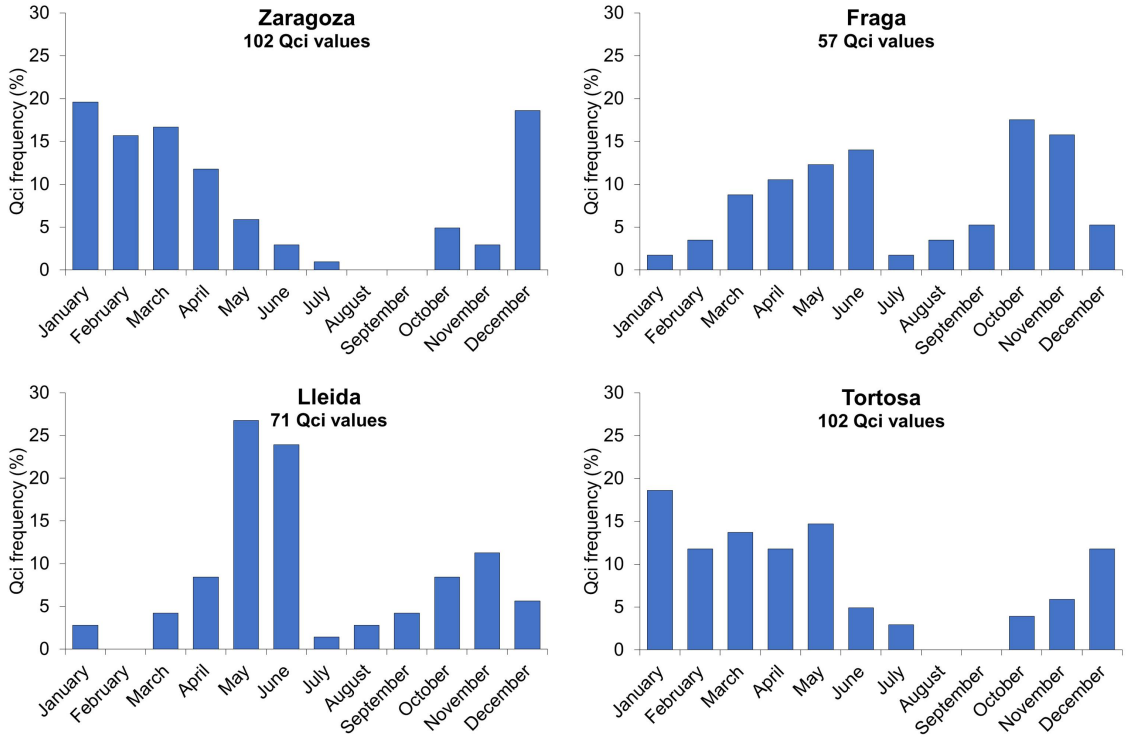

Figure 3. a) Etching of the 1871 flood at Zaragoza, where the Stone Bridge can be taken as a reference for the hydraulic reconstruction; b) post card of the Cinca River at Fraga during the 1930 flood showing the dimensions of the wall protecting the left side; c) flood mark at Camps Elisis in Lleida, used for the reconstruction of the 1907 flood; and d) scale on the Sant Martí church wall in Xerta, where the 9 highest water marks are indicated. Sources: a) Municipal Archives of Zaragoza; b) Fototipia Thomas de Barcelona, 1930; c) courtesy of R. Batalla; d) courtesy of A. Sánchez.

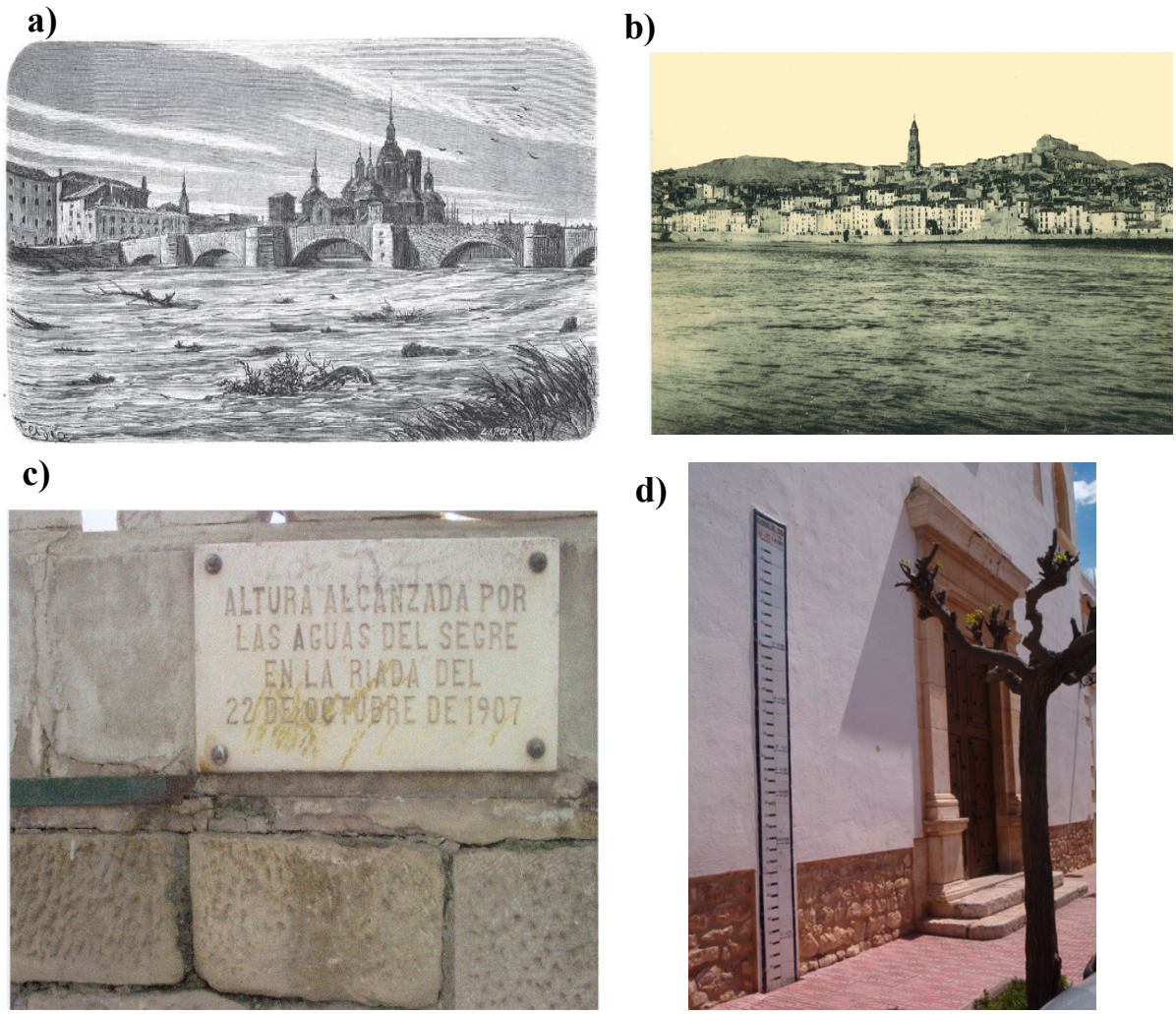

Figure 4. Non-systematic and systematic series of peak discharges (Qci) at a) Zaragoza, b) Fraga, c) Lleida, and d) Tortosa. The threshold for major floods is indicated for each site by a red horizontal line. Years between brackets indicate second order floods. At Tortosa, we have included secondary floods just below the threshold, whose magnitude is unknown but lower than 4500 m^3s^{-1}.

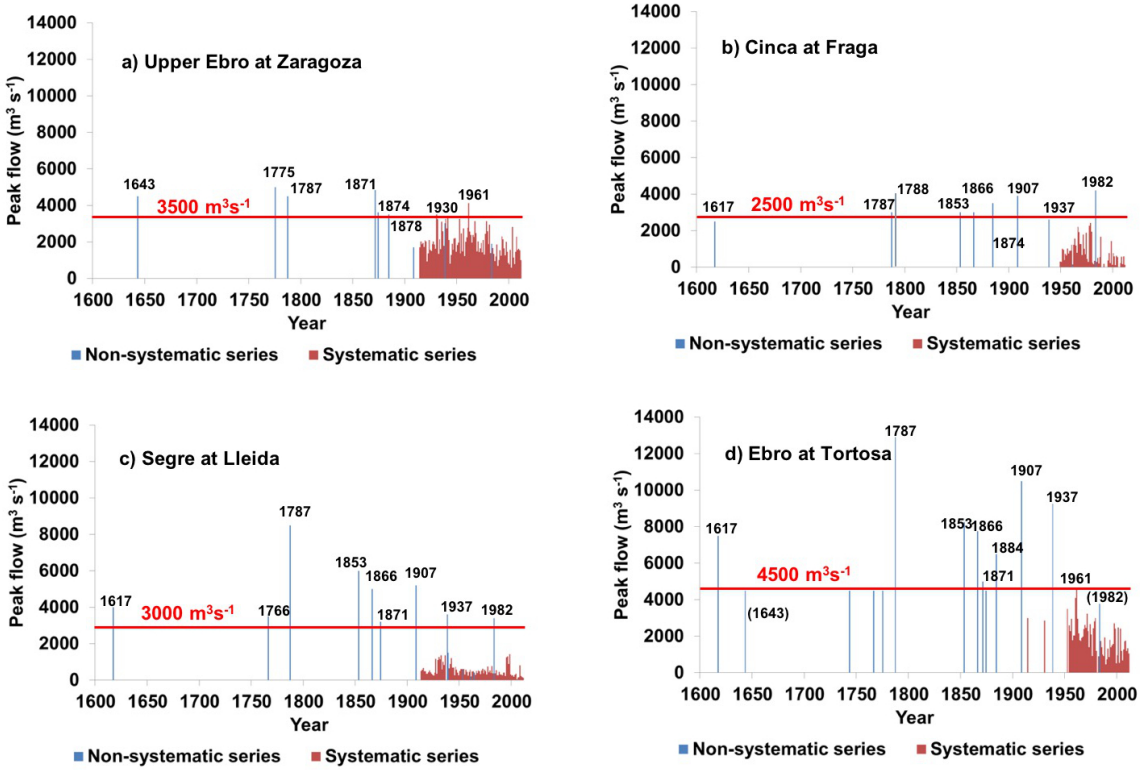

Figure 5. Month of occurrence of major floods for the Ebro at Zaragoza, the Cinca at Fraga, the Segre at Lleida, and the Ebro at Tortosa.